Modeling Complex Phase Transformations in Solidification Phenomena Using The Phase Field Crystal (PFC) Methodology

Nikolas Provatas
Department of Physics and Centre for the Physics of Materials
McGill University

VTT, Sept 13, 2017

Length and Time Scales in Materials Science

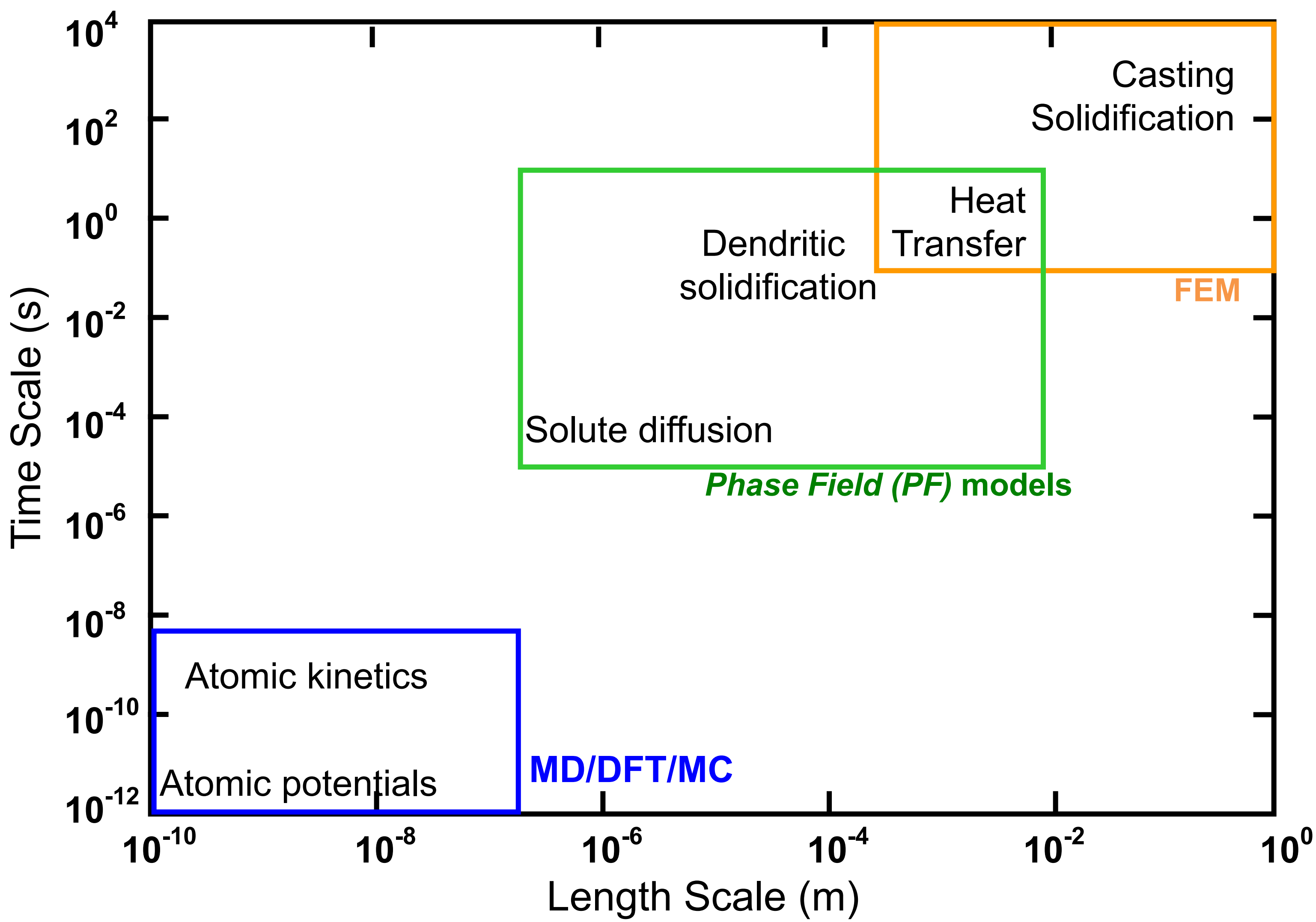

Multi-Phase & Multi-Component Solidification

$$\tau_\alpha \frac{\partial \phi_\alpha}{\partial t} = W_\alpha^2 \boldsymbol{\nabla}^2 \phi_\alpha - f'_{\mathrm{DW}}(\phi_\alpha) - w_{obs}\phi_\alpha \sum_{\beta\neq\alpha}^{N} \phi_\beta^2 - \left(\frac{(\boldsymbol{I} - [\boldsymbol{K}^\alpha])^T}{2} \vec{U}_\alpha + \hat{n}_c \right)^T [\lambda_\alpha]\, \vec{U}_\alpha\, g'_\alpha(\vec{\boldsymbol{\phi}})$$

$$[\boldsymbol{\chi}] \frac{\partial \vec{\mu}}{\partial t} = \boldsymbol{\nabla} \cdot \left[[\boldsymbol{M}] \boldsymbol{\nabla} \vec{\mu} + \sum_\alpha W_\alpha a(\vec{\boldsymbol{\phi}}) \, |\Delta \vec{C}_{\mathrm{eq}}^\alpha| \left\{ \hat{n}_c + (\boldsymbol{I} - [\boldsymbol{K}^\alpha])^T \vec{U}_\alpha \right\} \frac{\partial \phi_\alpha}{\partial t} \frac{\boldsymbol{\nabla}\phi_\alpha}{|\boldsymbol{\nabla}\phi_\alpha|} \right]$$

$$+ \frac{1}{2} \sum_\alpha |\Delta \vec{C}_{\mathrm{eq}}^\alpha| \left\{ \hat{n}_c + (\boldsymbol{I} - [\boldsymbol{K}^\alpha])^T \vec{U}_\alpha \right\} \frac{\partial \phi_\alpha}{\partial t},$$

$$\vec{U}_\alpha = \frac{[\boldsymbol{\chi}^L]}{|\Delta \vec{C}_{\mathrm{eq}}^\alpha|} (\vec{\mu} - \vec{\mu}_\alpha^{\mathrm{eq}})$$

$$\hat{n}_c = \frac{\Delta \vec{C}_{\mathrm{eq}}^\alpha}{|\Delta \vec{C}_{\mathrm{eq}}^\alpha|}$$

$$[\boldsymbol{K}^\alpha] = [\boldsymbol{\chi}^L]^{-1} [\boldsymbol{\chi}^\alpha]$$

$$[\lambda_\alpha] = \hat{\lambda}_\alpha |\Delta \vec{C}_{\mathrm{eq}}^\alpha|^2 [\chi^L]^{-1}$$

$$\Delta \vec{C}_{\mathrm{eq}}^\alpha = \vec{c}_{\mathrm{eq}}^{\,L} - \vec{c}_{\mathrm{eq}}^{\,\alpha}$$

$\phi_\alpha \leftarrow$ grain of solid α

$\vec{\mu} \leftarrow$ chemical potential

$\vec{\mu}_\alpha^{\mathrm{eq}} \leftarrow$ chemical potential of liquid $-\,\alpha$ equilibrium

$[\chi^\theta] \leftarrow$ inverse hessian of phase $\theta(\alpha, \mathrm{L})$

$\vec{c}_{\mathrm{eq}}^{\,\theta} \leftarrow$ equilibrium concs. of phase $\theta(\alpha, \mathrm{L})$

$$[\boldsymbol{\chi}] = [\boldsymbol{\chi}^L] \left\{ \mathbf{I} - \sum_\alpha \left(\mathbf{I} - [\boldsymbol{K}^\alpha] \right) h_\alpha(\vec{\phi}) \right\}$$

$$[\boldsymbol{M}] = \sum_\alpha^N q_\alpha(\vec{\boldsymbol{\phi}}) [\boldsymbol{D}]^\alpha [\boldsymbol{\chi}^\alpha] + \left(1 - \sum_\alpha^N q_\alpha(\vec{\boldsymbol{\phi}}) \right) [\boldsymbol{D}^L] [\boldsymbol{\chi}^L]$$

$g_\alpha(\vec{\phi}), h_\alpha(\vec{\phi}), q_\alpha(\vec{\phi}) \leftarrow$ interpolate between α & L

$[D^\theta] \leftarrow$ diffusivity of, phase $\theta(\alpha, \mathrm{L})$

Multi-Scale Challenges: Adaptive Mesh Refinement

Metal Powder

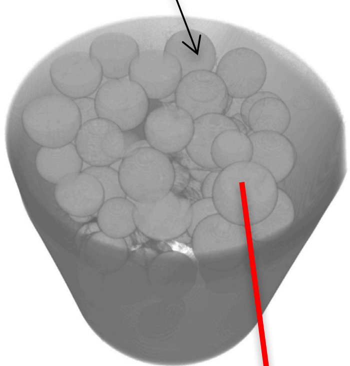

experiment

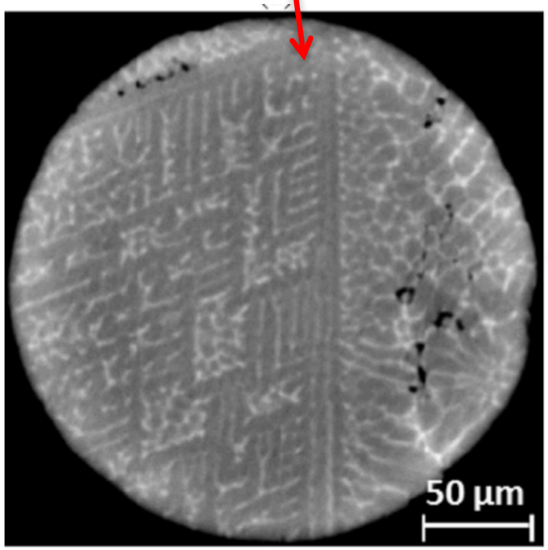

2D cross section: C.A. Gandin, H. Henein, and coworkers, Acta Mat. Vol. 89 (2015)

3D PF simulation

- **Equivalent uniform mesh**: ~10^10 nodes, 10^2 days of simulation
- **New 3D AMR mesh: ~**10^8 nodes and 65 hours of simulation (64 cores)

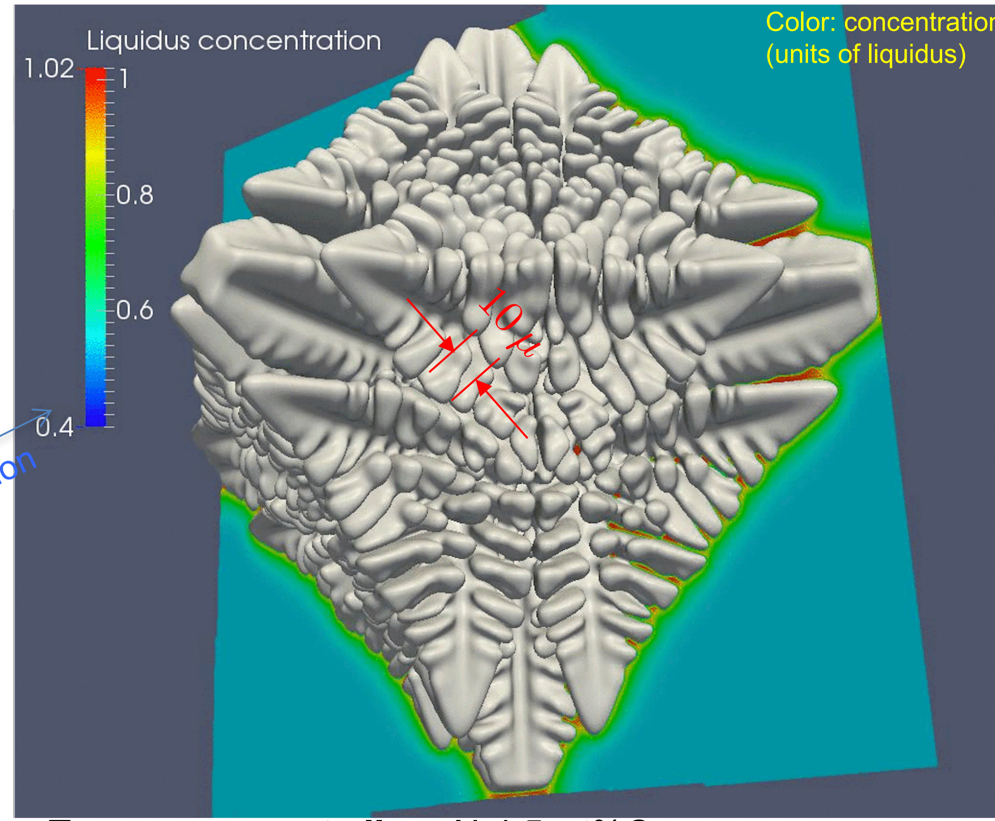

Two-component alloy: Al-4.5 wt%Cu
System (drop) size: ~100 um
Rapid quench to T=640 C

Grey: interface

[M. Greenwood, Raj Shampour, L. Wang, Nana Ofori-Opoku, T. Pinnoma and N. Provatas, J. Materials Science, in review (2017)

Noise-Induced Two-Phase Nucleation

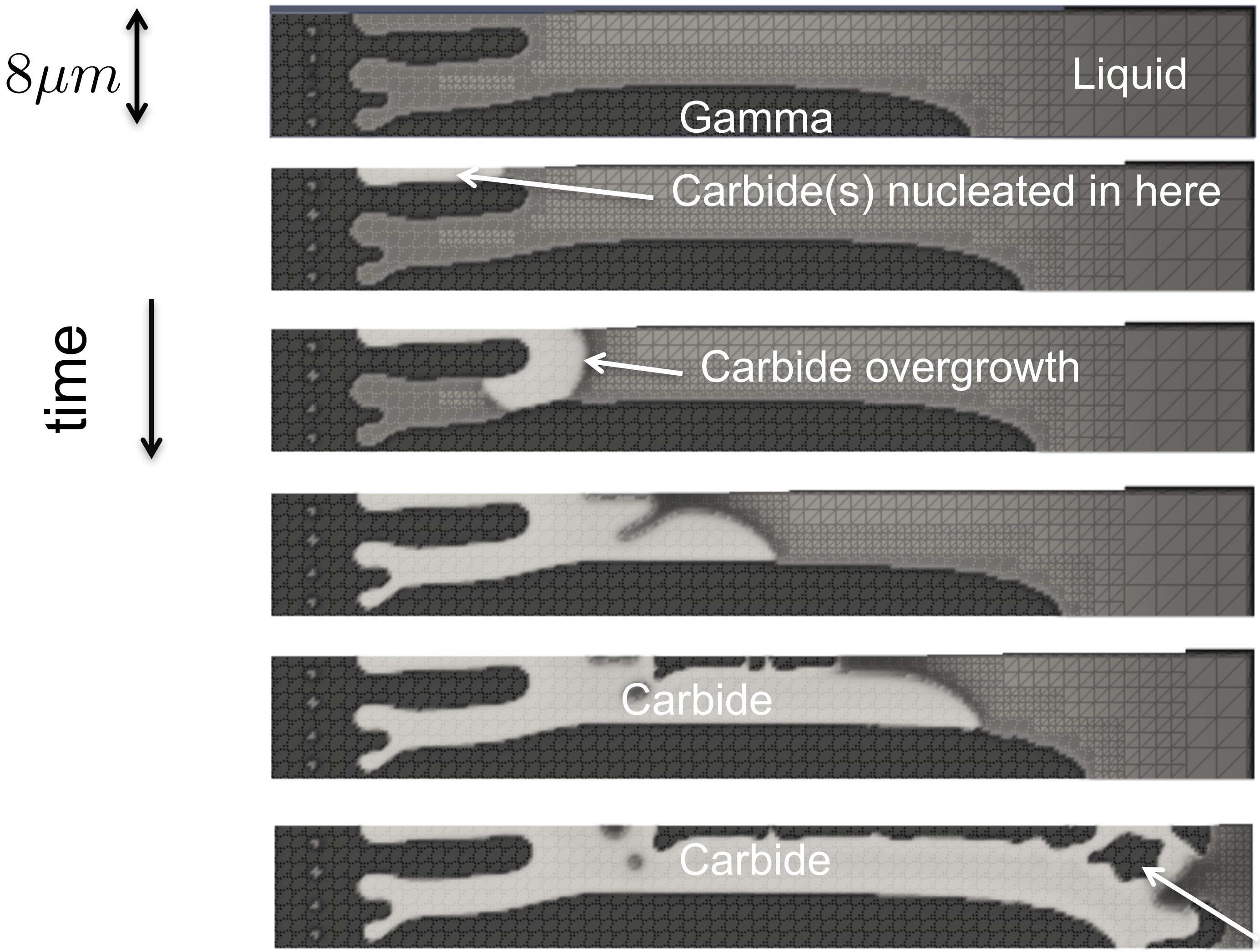

Thermal Gradient across mushy zone

$$G = 1 \times 10^6 K/m$$

Front speed

$$V = 5mm/s$$

*Nucleation occurred due to thermal fluctuations

Bridging a Gap in Scales

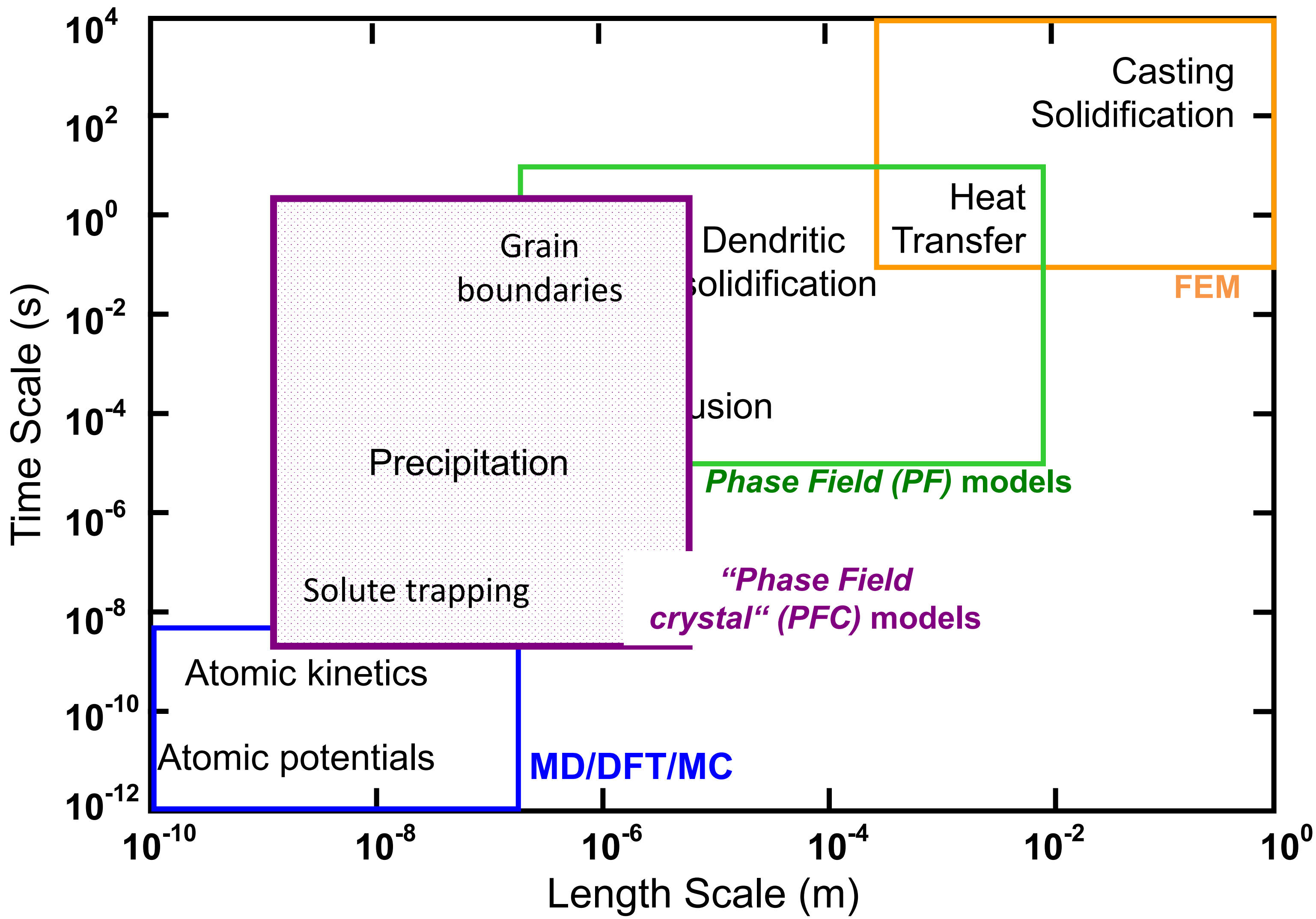

Modelling Atomic Effects in Crystallization and Solid State Transformations

Liquid

$\rho_m(r)$

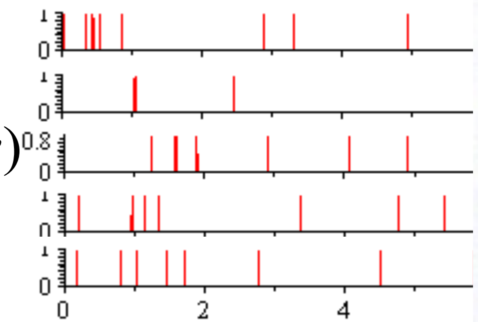

$\rho(r)$

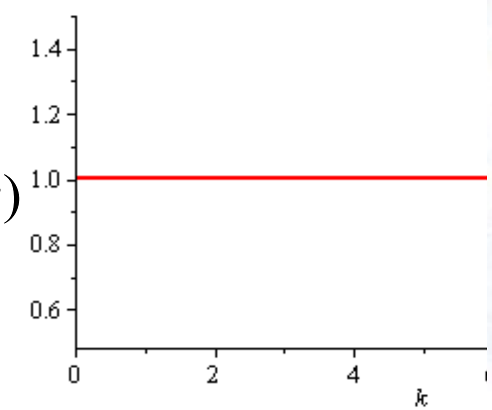

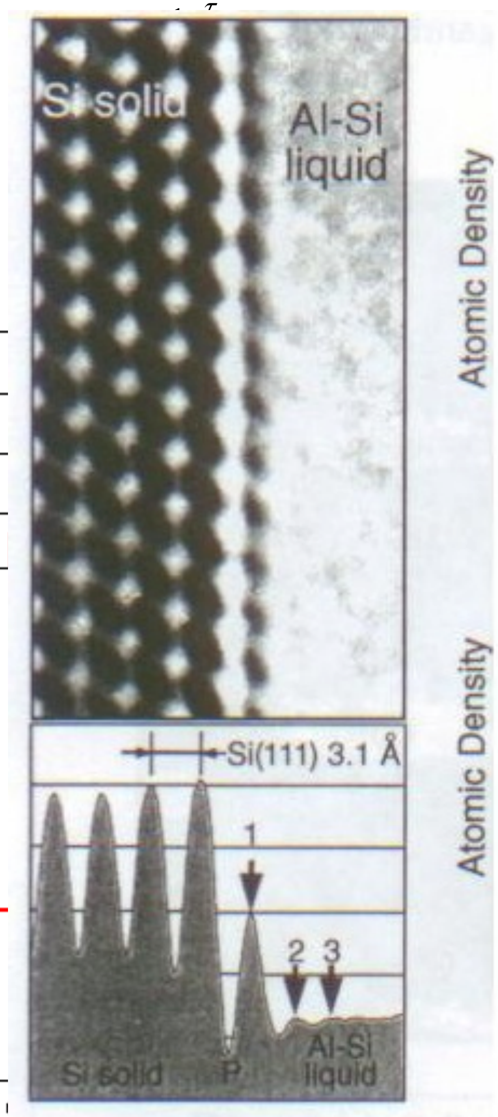

PL 2008

Solid

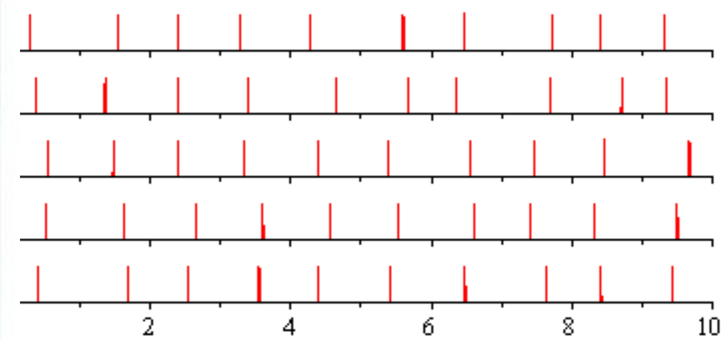

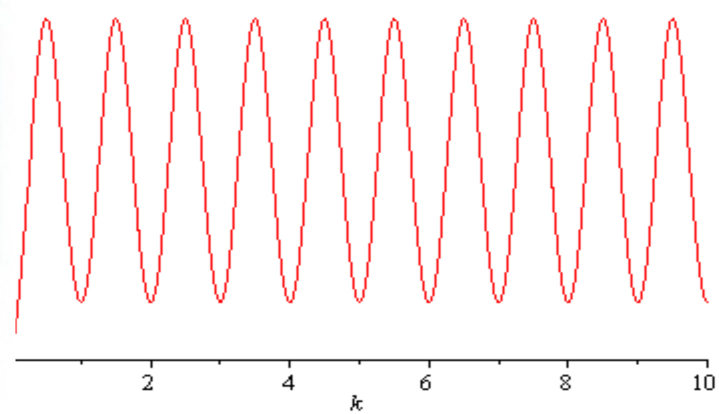

From cDFT to Phase Field Crystal (PFC) Methods

$$\frac{F}{k_B T} = F_{\mathrm{id}} + F_{\mathrm{int}}$$

$$\frac{F_{\mathrm{id}}}{k_B T \rho_o} \approx \int d\vec{r} \left(\frac{n^2}{2} - \frac{n^3}{3} + \frac{n^4}{12} \right) \qquad \frac{F_{\mathrm{int}}}{k_B T \rho_o} \approx \frac{1}{2} \iint d\vec{r}_2 d\vec{r}_2 n(\vec{r}_1) C_2(|\vec{r}_1 - \vec{r}_2|) n(\vec{r}_2)$$

$$n = (\rho - \rho_o)/\rho_o$$

$n(\vec{x})$ Varies at the atomic scale

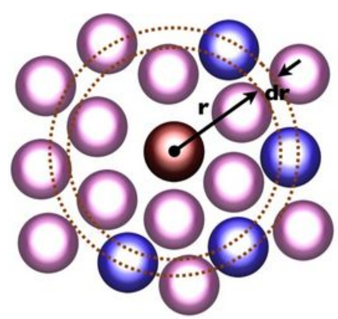

Frequency space view

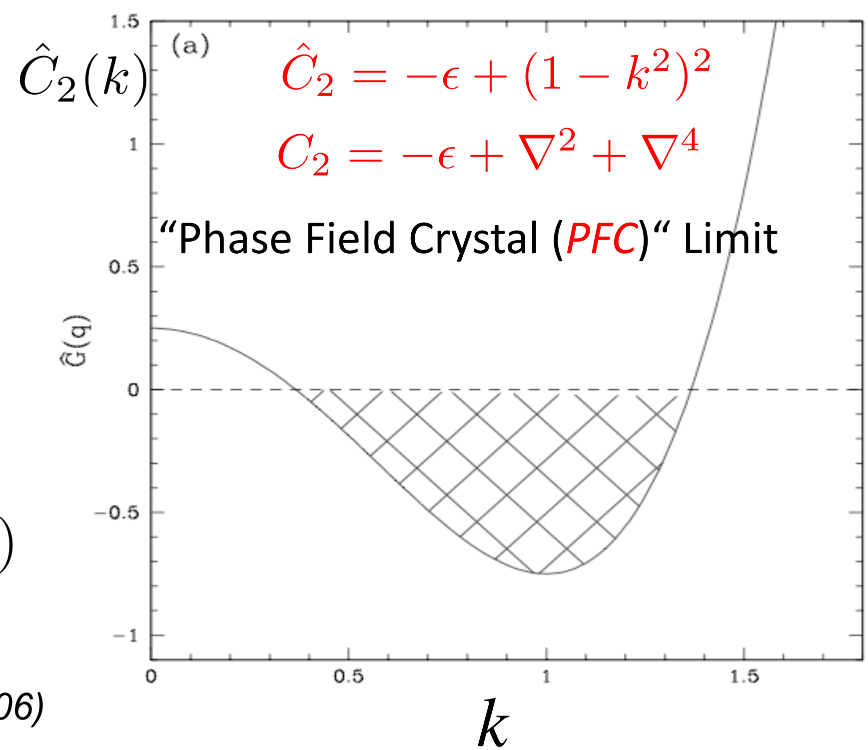

Density (n) Evolution

$$\frac{\partial^2 n}{\partial t^2} + \frac{1}{\beta} \frac{\partial n}{\partial t} = M \nabla^2 \left(\frac{\delta F}{\delta n} \right) + \eta(\mathbf{r}, t)$$

P. Stefanovic, M Hataaja and N. Provatas Phys. Rev. Lett (2006)

Complex Metal Structures: The "XPFC" Model

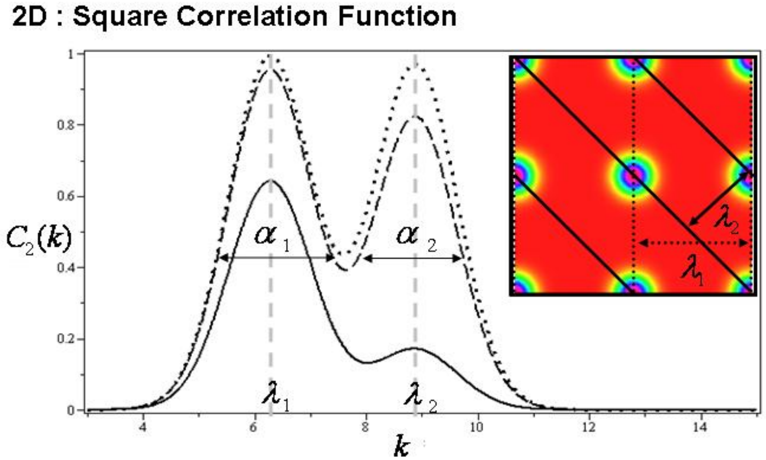

$$\hat{C}_2(k) = -r + \sum_i e^{\frac{\sigma(T) k_i^2}{2\rho_i \beta_i}} \; e^{-\frac{(k-k_i)^2}{2\alpha_i^2}}$$

2D: HCP, SC
3D: FCC, BCC, HPC, …

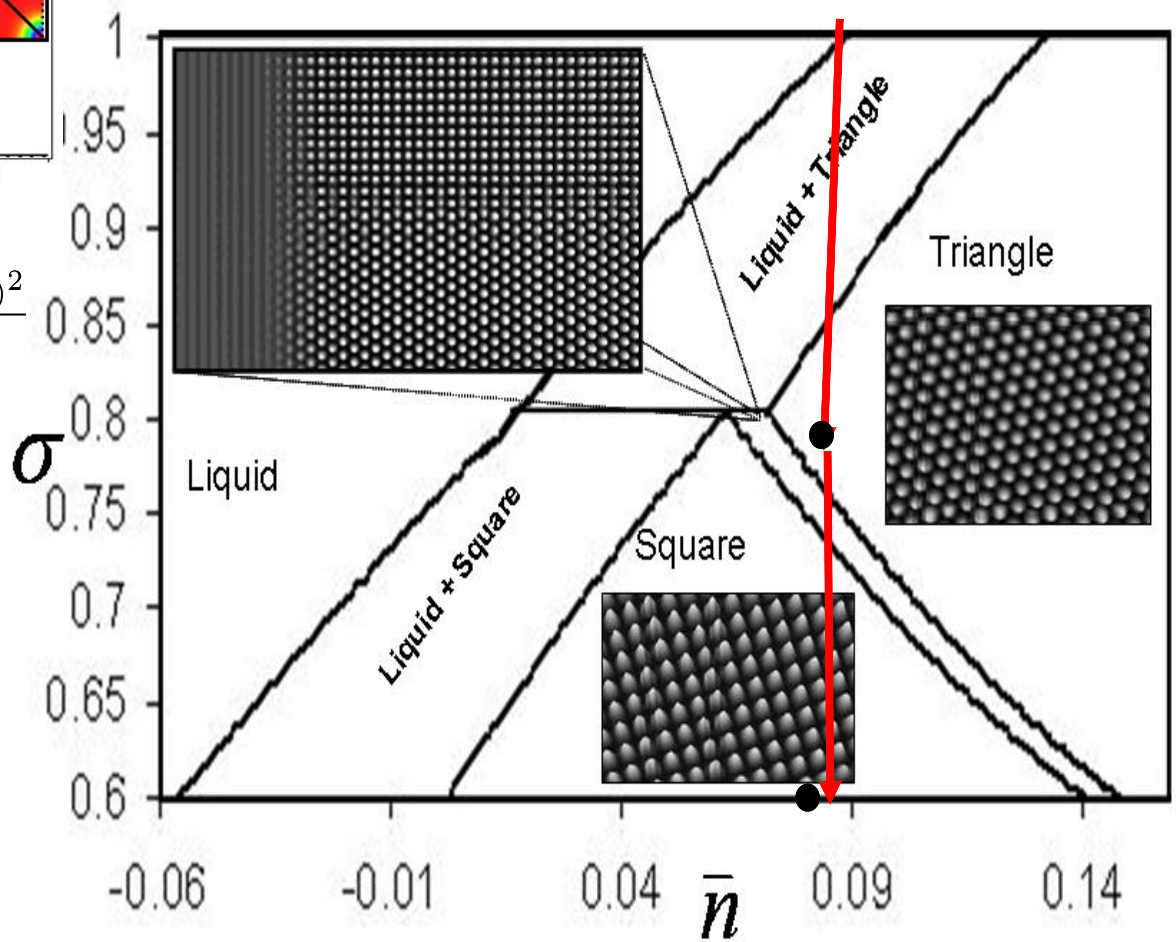

M. Greenwood, N. Provatas, J. Rottler, Phys. Rev. Lett, Vol. 105 (2011)

Metal Structures: The "XPFC" Model

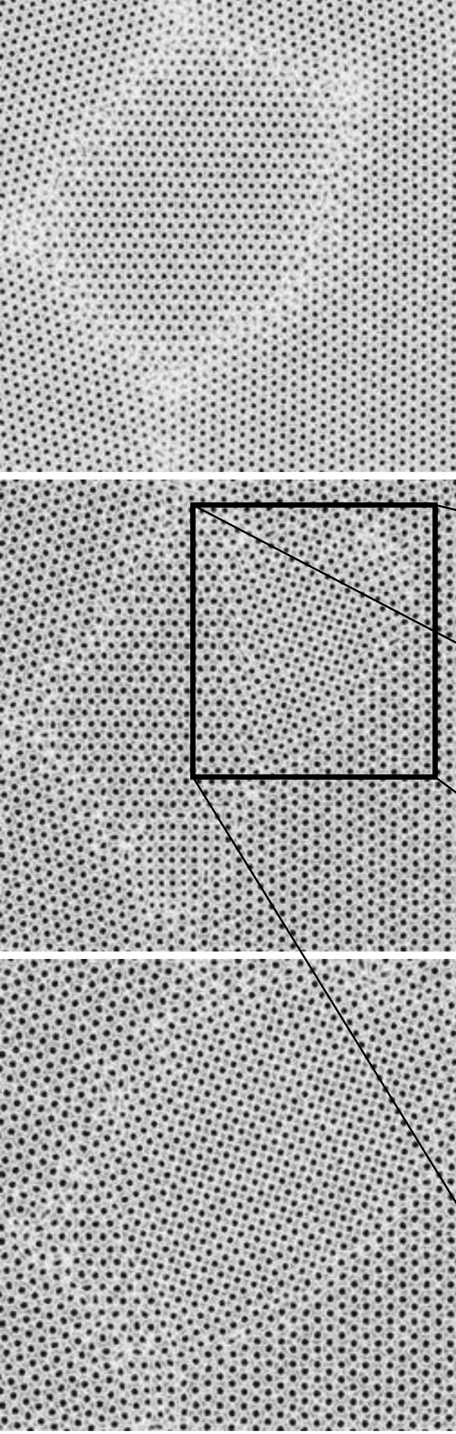

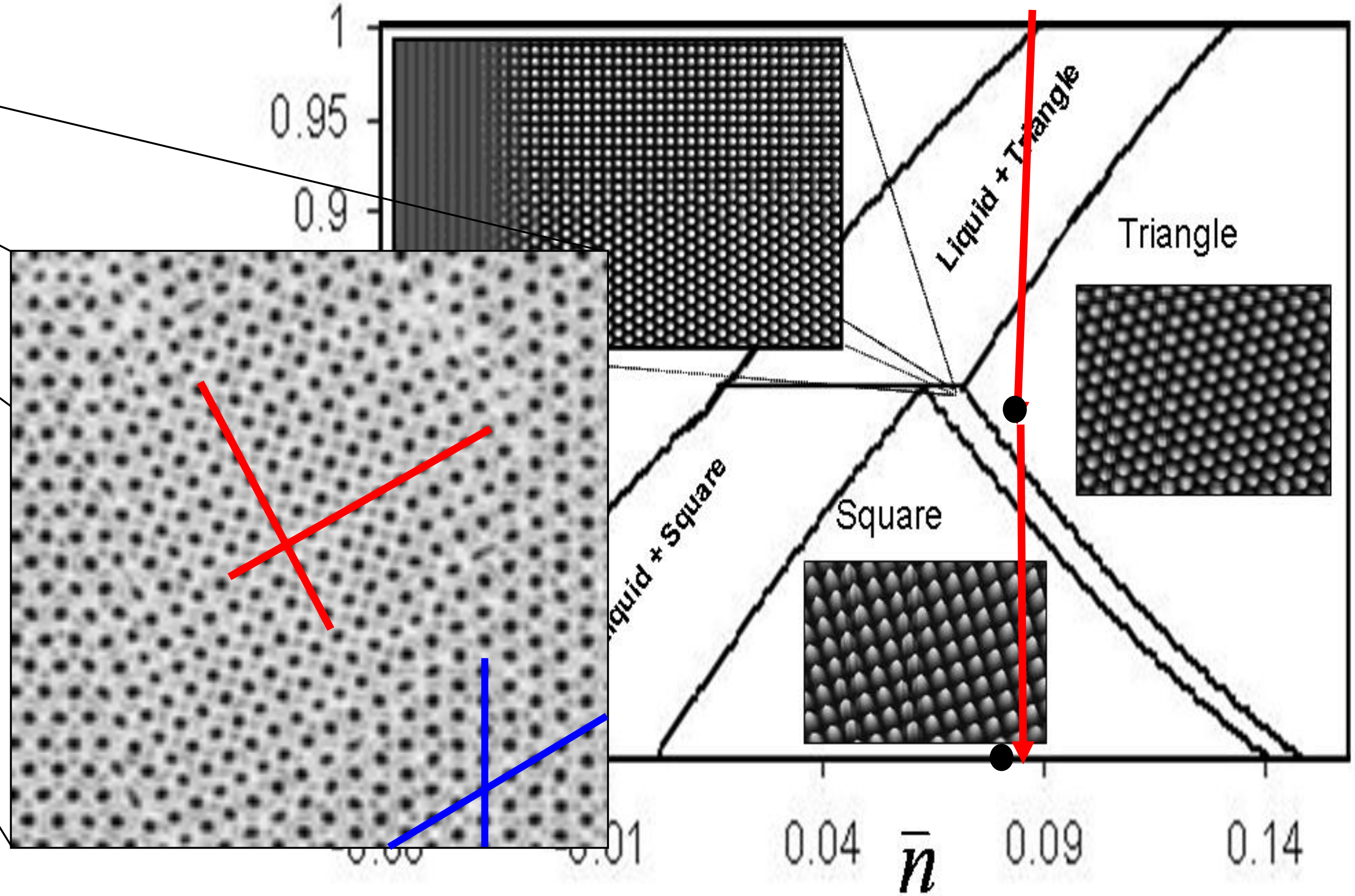

M. Greenwood, N. Provatas, J. Rottler, Phys. Rev. Lett, Vol. 105 (2011)

Conservative Dislocations (3D) Creation Mechanisms

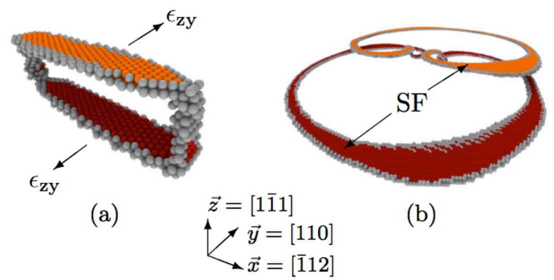

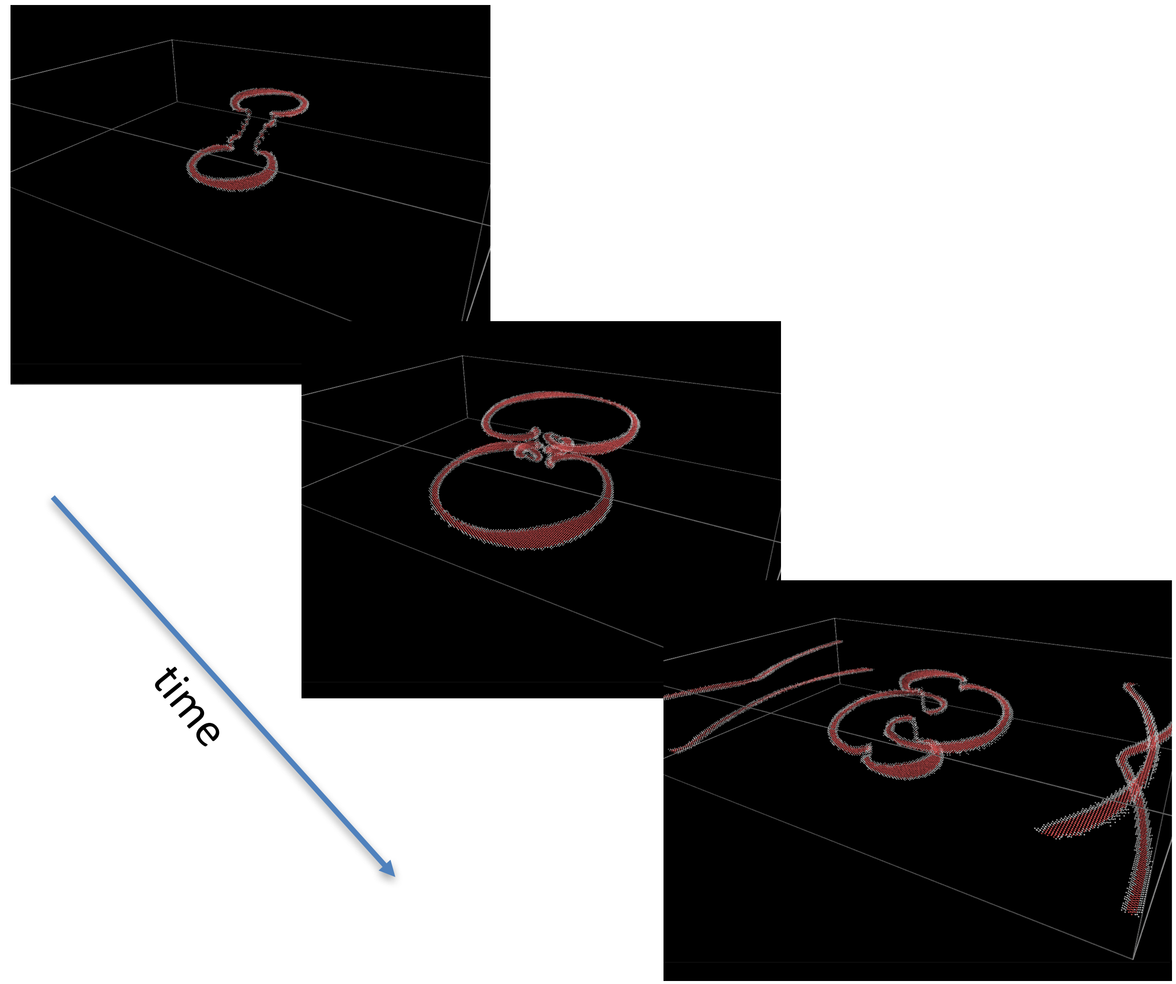

$$D_v^{Cu} = 10^{-13}\ m^2/s$$

$$\tau = 1.3\mu s$$

$$\dot{\epsilon}_{zy} = 180/s$$

Similar Structures by MD: M. de Koning, et al Phys. Rev. Lett. **91** (2003).

Joel Berry, N. Provatas, J. Rottler, C. Sinclair, Phys. Rev. B, Vol. 89 (2014)

XPFC Model of Multi-Component Alloys

$$\mathcal{F}_{id} = \sum_{i=1}^{N} \int \left\{ \rho_i \ln\left(\rho_i/\rho_i^o\right) - \left(\rho_i - \rho_i^o\right) \right\} d\mathbf{r}$$

$$\mathcal{F}_{\text{int}} = -\frac{1}{2} \sum_{i=1}^{N} \int \int \left\{ \delta\rho_i(\mathbf{r})\ C_2^{ij}(|\mathbf{r}-\mathbf{r}'|)\ \delta\rho_i(\mathbf{r}') \right\} d\mathbf{r}\, d\mathbf{r}'$$

$$n = \rho_1 + \rho_2 + \cdots$$

$$c_i = \rho_i / \left(\sum_{j=1}^{N} \rho_j \right)$$

$$C_{2(eff)} = \sum_i \chi_i\left(\{c_j\}\right) C_2^{ii}\left(|\mathbf{r}-\mathbf{r}'|\right)$$

$$\frac{\Delta F}{k_B T \rho_o} = \int \left\{ \frac{n^2}{2} + \xi\frac{n^3}{3} + \chi\frac{n^4}{4} - n(\mathbf{x}) \left(\int C_{2(eff)}(|\mathbf{x}-\mathbf{x}'|) n(\mathbf{x}) d\mathbf{x}' \right) + \Delta F_{mix}(\{c_i\})(n+1) + \frac{1}{2} \sum_{i,j=1}^{N} \kappa_{ij} \nabla c_i \cdot \nabla c_j \right\} d\mathbf{x}$$

N. Ofori-Opoku, et. al, Phys. Rev. B, Vol. 87, 134105 (2013)

Application: Dislocation –Mediated Nucleation of Precipitate Clusters in Al-Cu

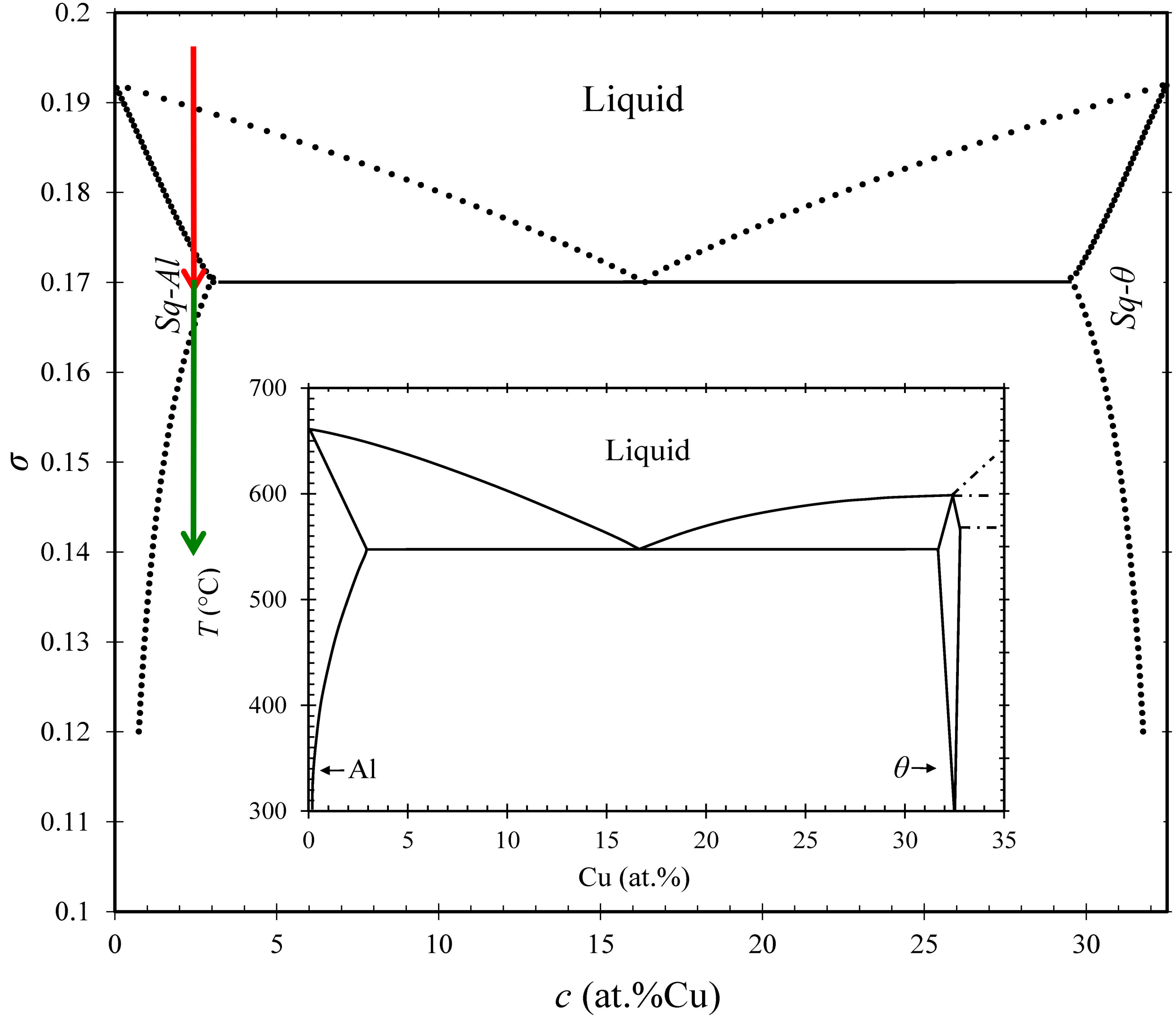

Fallah et. al, Phys Rev. B, Vol. 86, 134112 (2012)

Application: Dislocation –Mediated Nucleation of Precipitate Clusters in Al-Cu

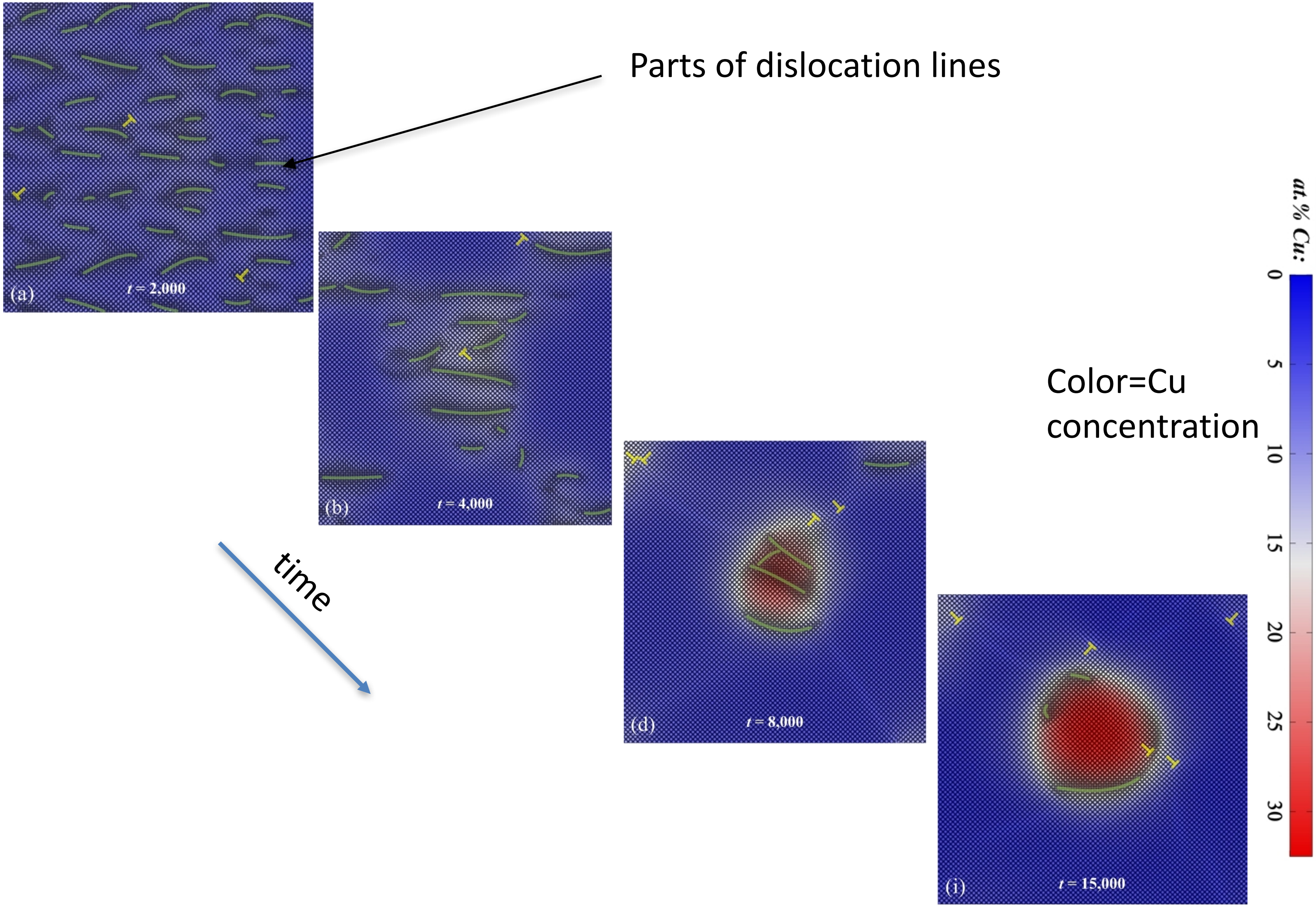

Fallah et. al, Phys Rev. B, Vol. 86, 134112 (2012)

The Role of Dislocations in Mediating Clustering

Work of formation: $\Delta W = 2\pi R\gamma + \pi R^2\left(\Delta f + \Delta G_{\mathrm{cs}}\right) - \psi^2\chi_d E A \ln(R) + \zeta A$

$$A = G_A \sum b_i^2 / 4\pi(1-\nu)$$

$$\psi^2\chi_d \equiv \frac{\psi_{Mg}\psi_{Mg}\frac{\partial^2 f}{\partial c_{si}^2} + \psi_{Si}\psi_{Si}\frac{\partial^2 f}{\partial c_{Mg}^2} + \psi_{Si}\psi_{Mg}\frac{\partial^2 f}{\partial c_{Mg}\partial c_{si}}}{\frac{\partial^2 f}{\partial c_{Si}^2}\frac{\partial^2 f}{\partial c_{Mg}^2} - \left(\frac{\partial^2 f}{\partial c_{Mg}\partial c_{si}}\right)}$$

F. Larche, J.W. Cahn, Acta Metall (1985).

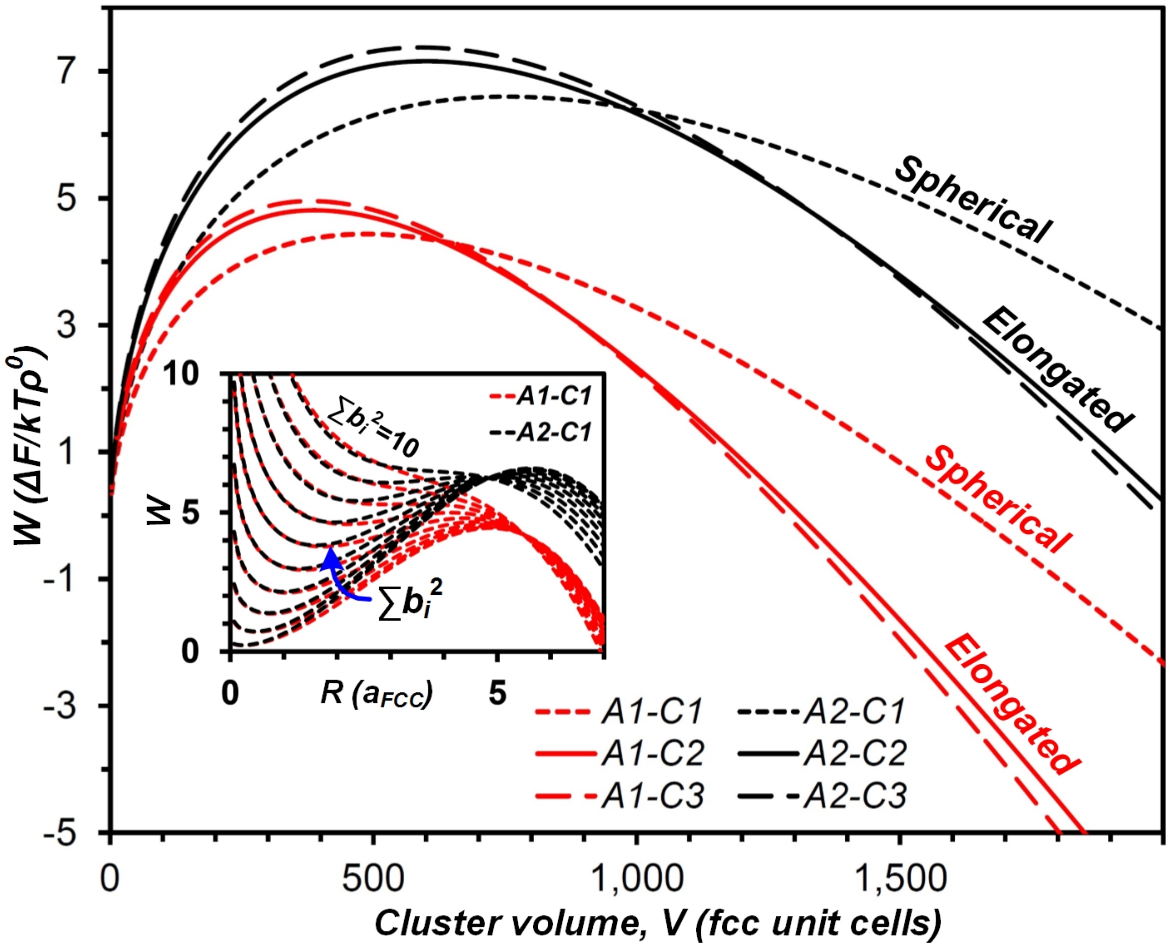

V. Fallah et. al, Acta Materialia, Vol. 82, (2015)

The Role of Dislocations in Mediating Clustering

F. Larche, J.W. Cahn,
Acta Metall (1985).

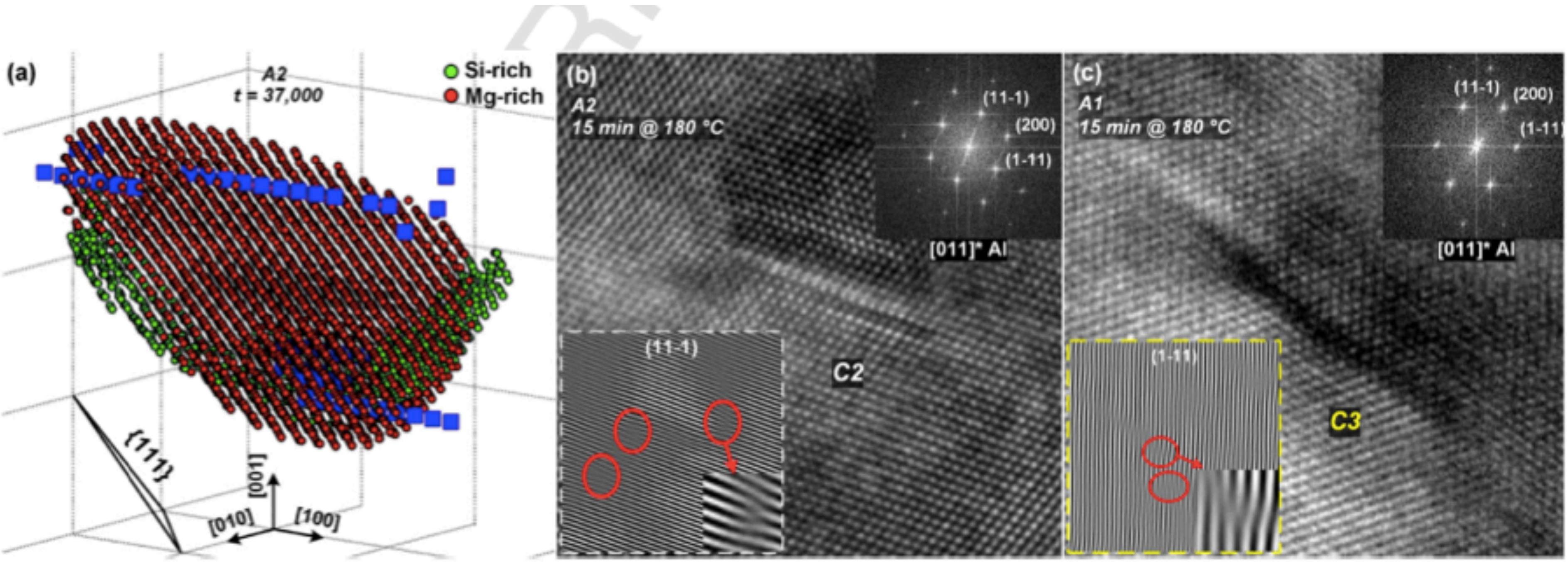

V. Fallah et. al, Acta Materialia, Vol. 82, (2015)

In partnership with Novelis Inc. and The Canadian Centre for Electron Microscopy at McMaster

Extending the PFC Approach to Three-Point Interactions: Non-Metallic Materials

$$\frac{\Delta F}{k_B T \bar{\rho}} = F_{id}[n] + F_{ex,2}[n] + F_{ex,3}[n]$$

$$\mathcal{F}_{id} \approx \int d(\mathbf{r}) \left\{ \frac{n^2}{2} - \nu \frac{n^3}{6} + \xi \frac{n^4}{12} \right\}$$

$$F_{ex,2} = -\frac{1}{2} \int n(\mathbf{r}) \int C_2(\mathbf{r} - \mathbf{r}')\ n(\mathbf{r}')\ d\mathbf{r}'\ d\mathbf{r}$$

$$\boxed{C_2(r) = -\frac{R}{\pi r_o^2}(r)\ \mathrm{circ}\left(\frac{r}{r_o}\right)}$$

Hard Sphere repulsion

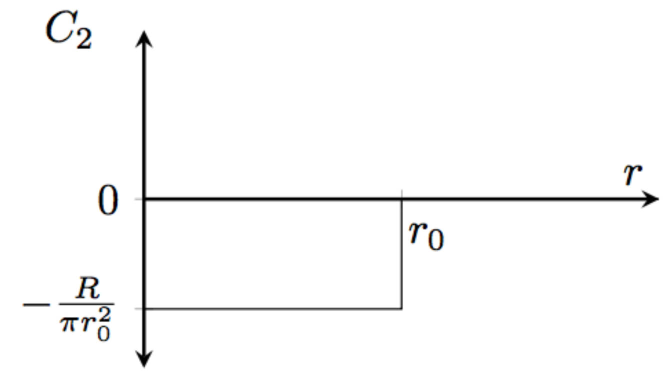

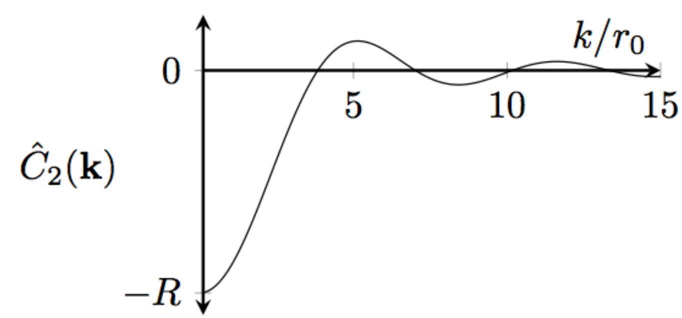

Rotationally Invariant 3-Point Correlation Function or Graphene

$$F_{ex,3} = -\frac{1}{3}\int n(\mathbf{r}) \int C_3(\mathbf{r}-\mathbf{r}', \mathbf{r}-\mathbf{r}'')\; n(\mathbf{r}')n(\mathbf{r}'')d\mathbf{r}'\, d\mathbf{r}''\, d\mathbf{r}$$

$$\boxed{C_3(\mathbf{r}-\mathbf{r}', \mathbf{r}-\mathbf{r}'') = \sum_i C_s^{(i)}(\mathbf{r}-\mathbf{r}')C_s^{(i)}(\mathbf{r}-\mathbf{r}'')}$$

$$C_s^{(1)}(r,\theta) = C_r(r)C_\theta^{(1)}(\theta) = C_r(r)\cos(m\theta)$$

$$C_s^{(2)}(r,\theta) = C_r(r)C_\theta^{(2)}(\theta) = C_r(r)\sin(m\theta)$$

$$C_r(r) = X(T^{-1})2\pi a_o\delta(r-a_o)$$

$$\boxed{\sum_i C_s^{(i)}(\mathbf{r}-\mathbf{r}')C_s^{(i)}(\mathbf{r}-\mathbf{r}'') = C_r(\mathbf{r}-\mathbf{r}')C_r(\mathbf{r}-\mathbf{r}'')\cos\left(m(\theta_2-\theta_1)\right)}$$

*Rotationally Invariant

M. Seymour and N. Provatas, Phys. Rev. B Vol. 93, 035447 (2016)

Nucleation/Growth of Graphene Polycrystals

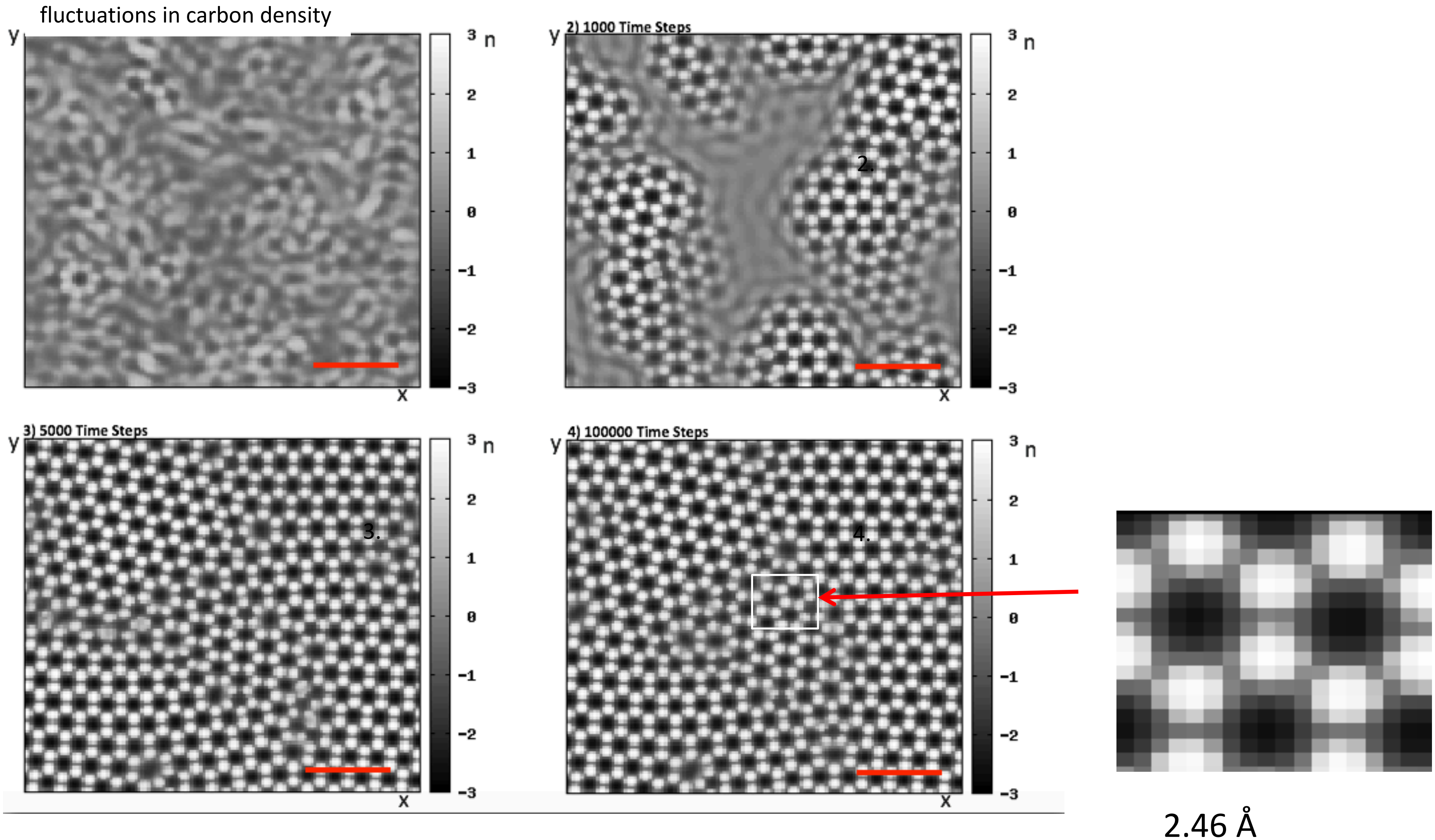

Red Bar = 7.38 Å

Kate Elder, MSc Thesis (2017)

Experimental Comparison of Defects

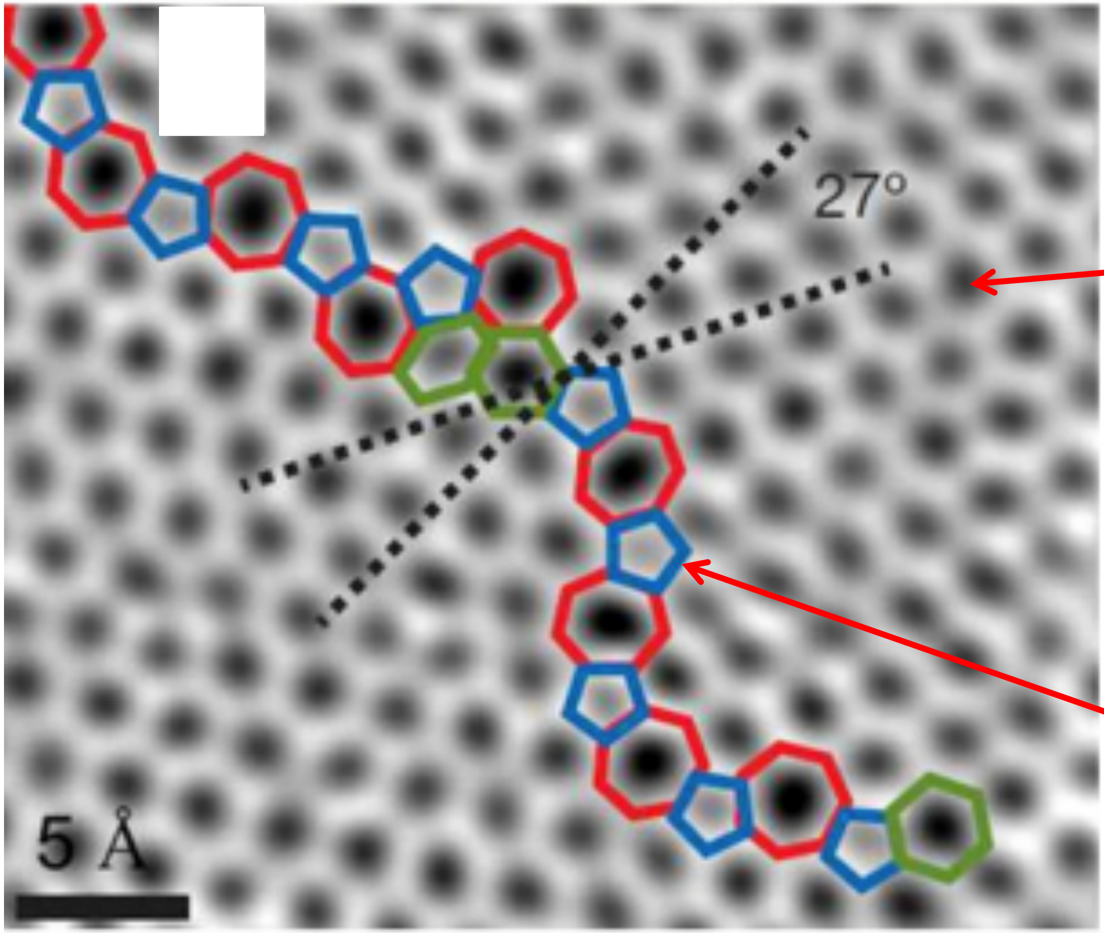

Experimental

Red – 7, Green – 6, Blue - 5

Normal Graphene

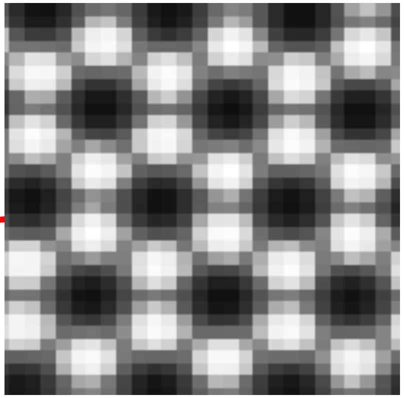

5-7 Defect

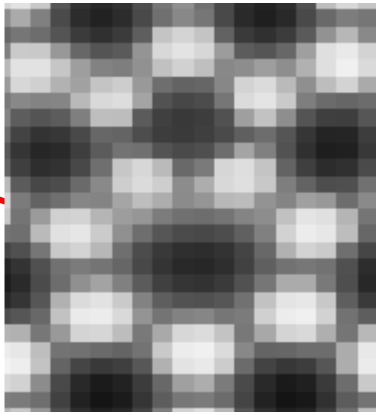

Terrones, H.; Lv, R.; Terrones, M.; Dresselhaus, M. The role of defects and doping in 2D graphene sheets and 1D nanoribbons. *Reports on Progress in Physics.* **75**, 062501 (2012).

Contoliing Long-Range Particle Interactions: PFC Modelling of Vapour-Liquid-Solid Systems

$$\frac{\Delta F}{k_B T \bar{\rho}} = F_{VdW}[n] + F_{ex,2}[n]$$

$$F_{VdW}[\rho] = F_{id} - \int d\mathbf{r} \left[\rho_{mf} \ln(1 - \rho_{mf} b) + \frac{a}{k_B T} \rho_{mf}^2 \right]$$

Modified Van der Walls Interaction

$$\rho_{mf}(\mathbf{r}) = \int d\mathbf{r} \chi(\mathbf{r} - \mathbf{r}') \rho(\mathbf{r})$$

$$\chi(k) = \exp(-k^2/(2\lambda))$$

G. Kocher and N. Provatas, Phys. Rev. Lett, Vol. 114 (2015)

Density Functional Theory with Long-Range Multi-Point Interactions

$$\mathcal{F}[n] = \int d\mathbf{r}\left[\frac{n(\mathbf{r})^2}{2} - \frac{n(\mathbf{r})^3}{6} + \frac{n(\mathbf{r})^4}{12}\right]$$

$$-\frac{1}{2}\int d\mathbf{r}_1 d\mathbf{r}_2\, C_2(\mathbf{r}_1 - \mathbf{r}_2)\, n(\mathbf{r}_1)\, n(\mathbf{r}_2)$$

$$+\sum_{m=3}^{4}\frac{1}{m}\left(\int d\mathbf{r}_1 \cdots d\mathbf{r}_m\, \chi^{(m)}(\mathbf{r}_1 \cdots \mathbf{r}_m)\, n(\mathbf{r}_1)\cdots n(\mathbf{r}_m)\right)$$

$$\chi^{(3)} = (a\,r + b)\chi(\mathbf{r}_1 - \mathbf{r}_2)\,\chi(\mathbf{r}_1 - \mathbf{r}_3)$$

$$\chi^{(4)} = c\,\chi(\mathbf{r}_1 - \mathbf{r}_2)\,\chi(\mathbf{r}_1 - \mathbf{r}_3)\,\chi(\mathbf{r}_1 - \mathbf{r}_4)$$

$$\chi(k) = \exp(-k^2/(2\lambda))$$

Three-Phase Coexistence with a Single PFC Density Field

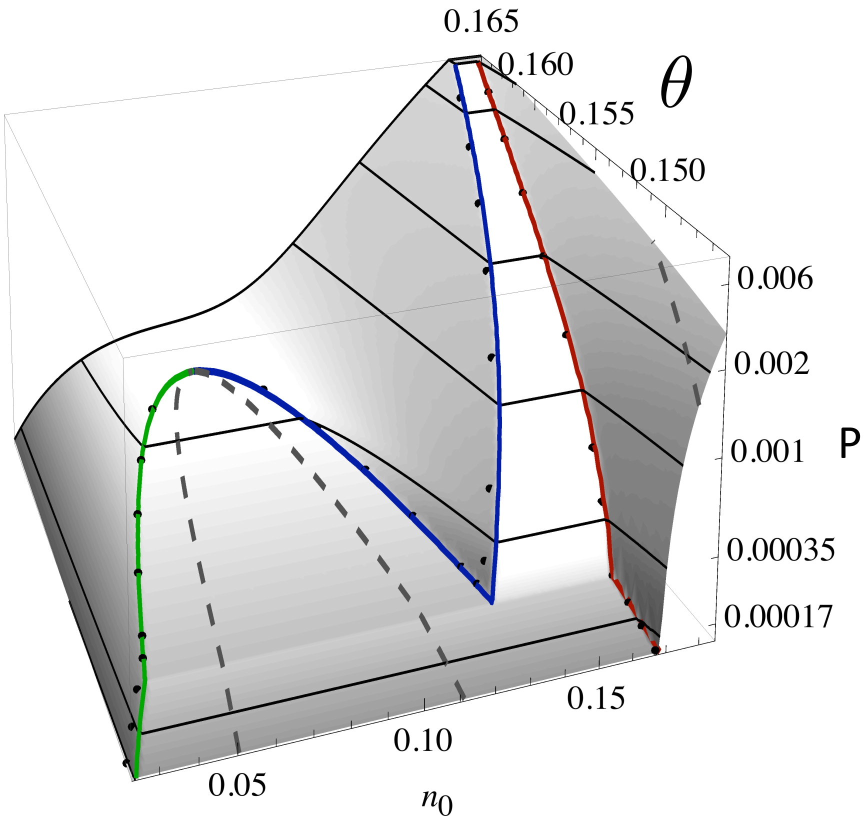

Crystal structure set by using:

$$\hat{C}_2(k) = -(r + (1-k^2)^2)$$

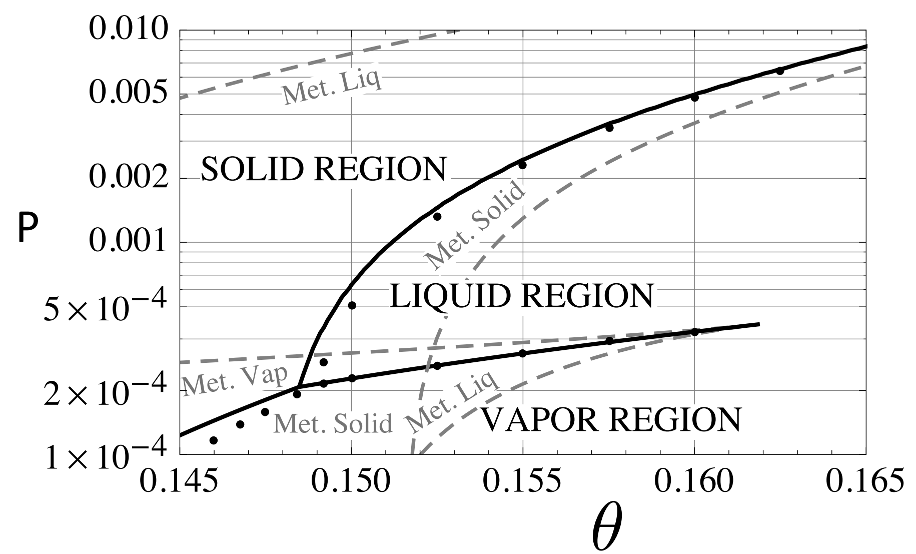

Crystallization of Liquid Via The Vapour Phase

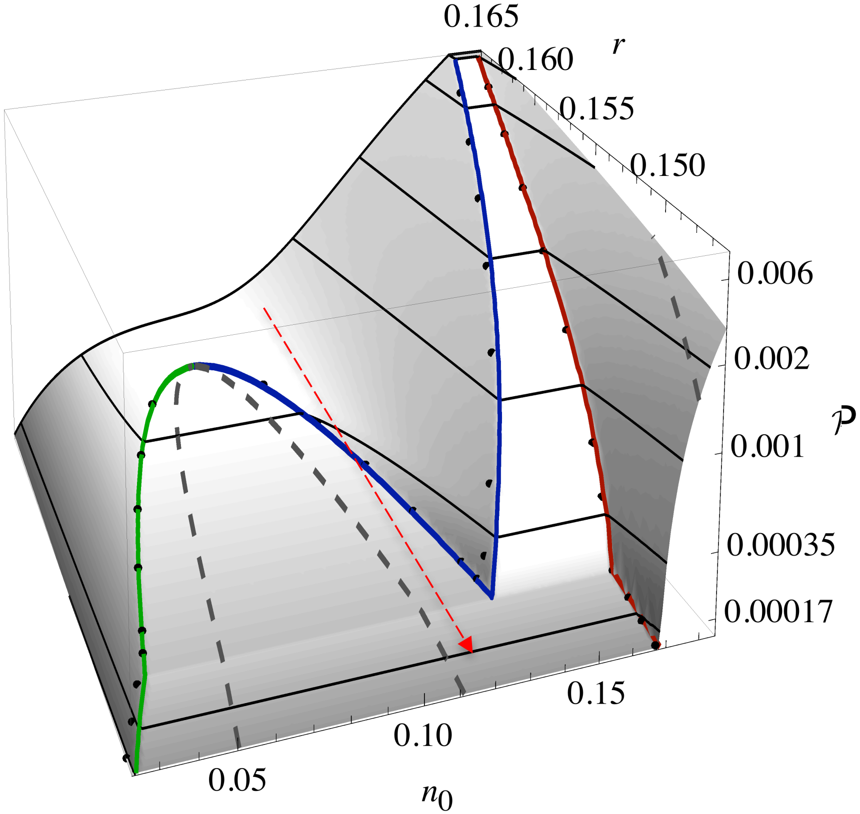

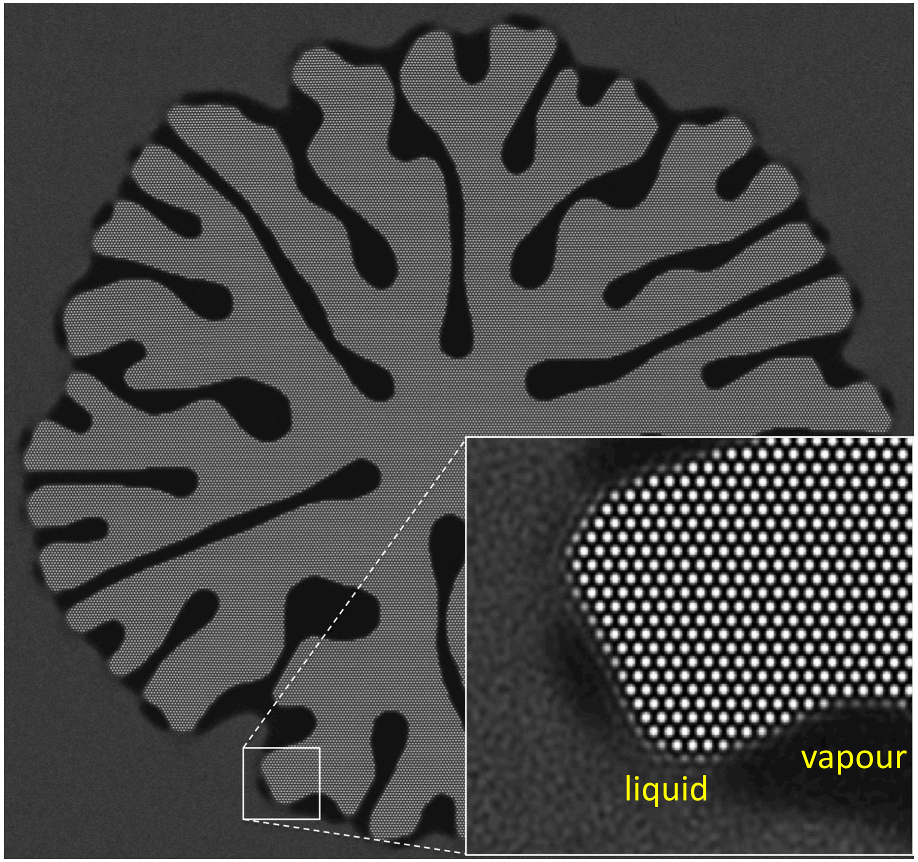

Application to Electromigration

$$\mathcal{F}[n] = \int d\mathbf{r} \left[\frac{n(\mathbf{r})^2}{2} - \frac{n(\mathbf{r})^3}{6} + \frac{n(\mathbf{r})^4}{12} \right]$$

$$-\frac{1}{2} \int d\mathbf{r}_1 d\mathbf{r}_2 \, C_2(\mathbf{r}_1 - \mathbf{r}_2) \, n(\mathbf{r}_1) \, n(\mathbf{r}_2)$$

$$+\sum_{m=3}^{4} \frac{1}{m} \left(\int d\mathbf{r}_1 \cdots d\mathbf{r}_m \, \chi^{(m)} \, (\mathbf{r}_1 \cdots \mathbf{r}_m) \, n(\mathbf{r}_1) \cdots n(\mathbf{r}_m) \right)$$

$$+\frac{A_o}{k_B T \bar{\rho}} \int q[n] V(r) dr \qquad q(r) = \frac{eZ^*}{\Omega} \langle n(r) \rangle n(r)$$

$$\frac{\partial n}{\partial t} = \nabla \cdot \left(\Gamma \nabla \frac{\delta \mathcal{F}}{\delta n} \right) + \eta \qquad \nabla \cdot (\sigma[n] \nabla V) = 0$$

Nan Wang, K. Bevan and N. Provatas, Phys. Rev. Lett. Vol. 117 (2016)

Void Growth and migration in Electromigration in Nanoelectronic Interconnects

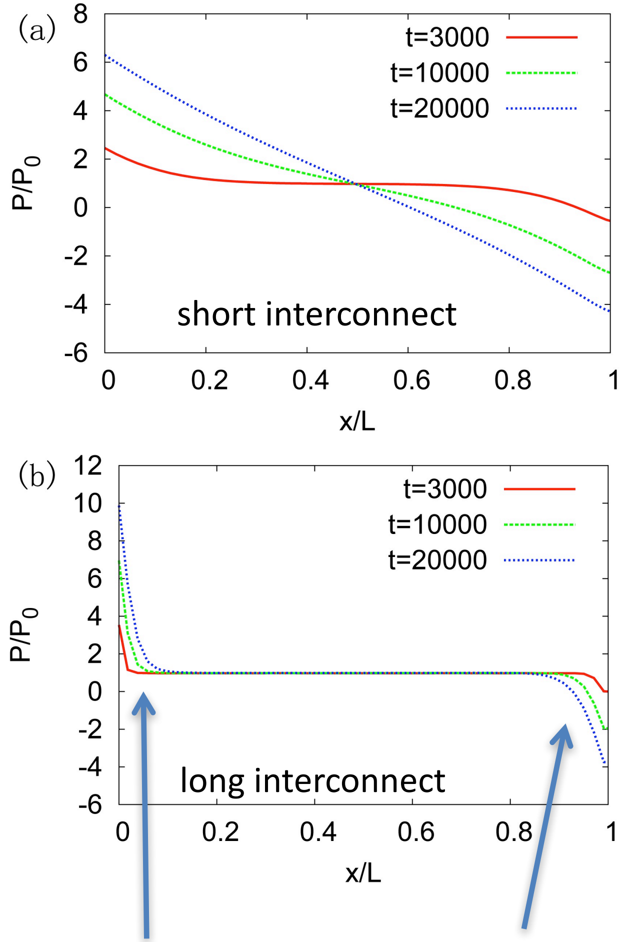

Atom buildup

Vacancy buildup

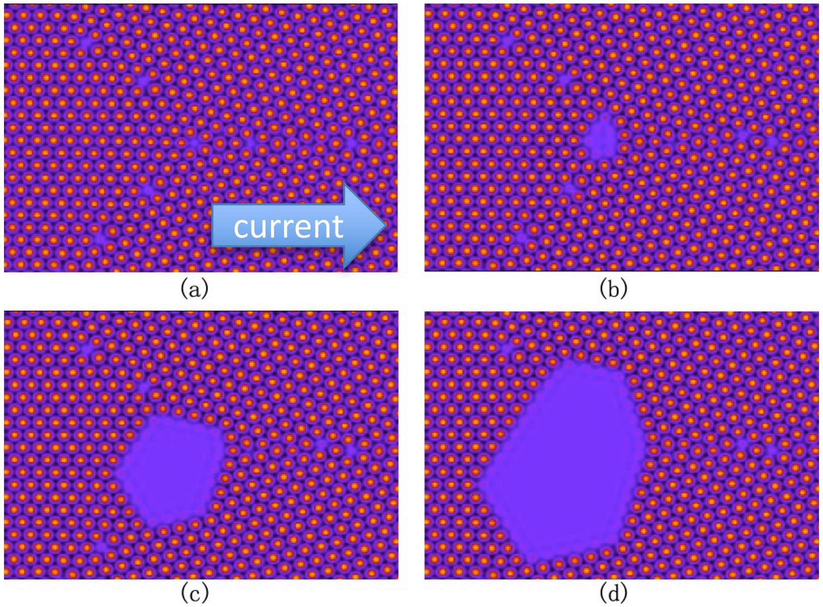

Time to void nucleation (failure)

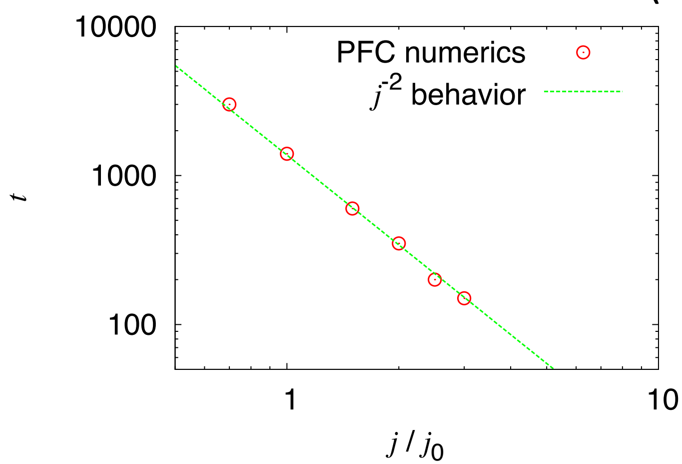

Blech Effect: I.A. Blech, J. Appl. Phys, 47 (1976)

M. Shatzkes and J.R. Lloyd, J. Appl. Phys, 59 (1986)

Void Deformation and Migration

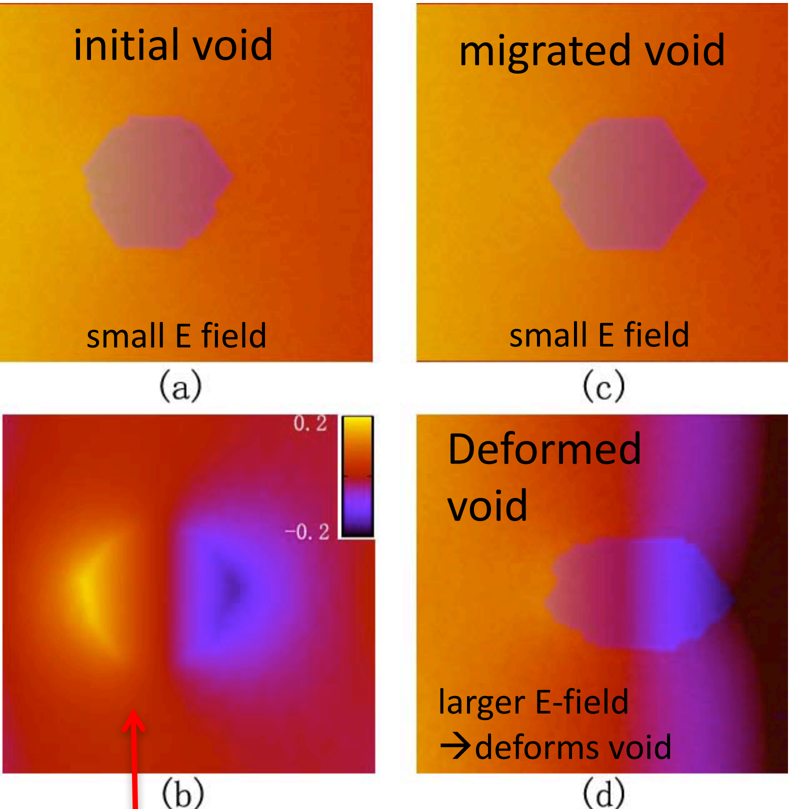

change of
potential in (a)

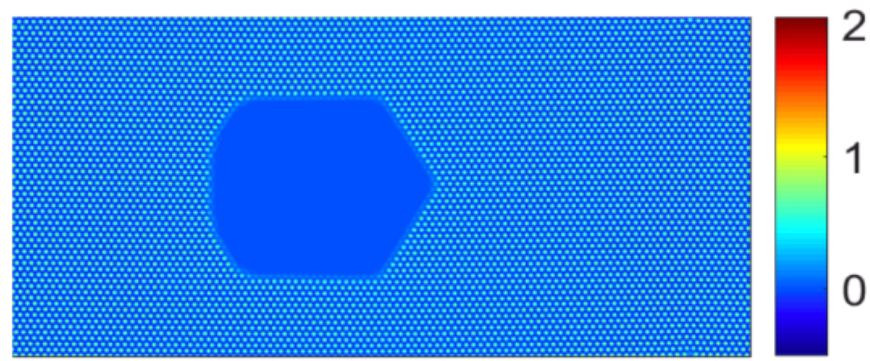

PFC simulation

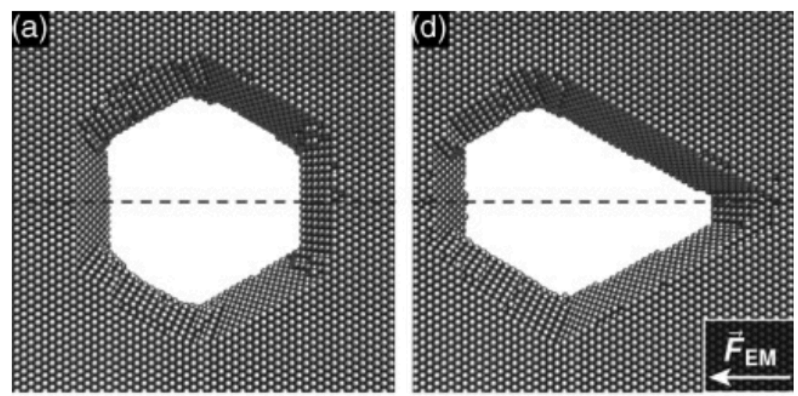

A. Latz et. al. Phys. Rev. B, **85** (2012)

Multi-Point Interactions in Alloys: Solidification Shrinkage & Cavitation

$$\mathcal{F}[n] = \int d\mathbf{r}\left[\frac{n(\mathbf{r})^2}{2} - \frac{n(\mathbf{r})^3}{6} + \frac{n(\mathbf{r})^4}{12}\right]$$
$$-\frac{1}{2}\int d\mathbf{r}_1 d\mathbf{r}_2\, C_{2(eff)}(\mathbf{r}_1 - \mathbf{r}_2)\, n(\mathbf{r}_1)\, n(\mathbf{r}_2)$$
$$+\sum_{m=3}^{4}\frac{1}{m}\left(\int d\mathbf{r}_1 \cdots d\mathbf{r}_m\, \chi^{(m)}\,(\mathbf{r}_1 \cdots \mathbf{r}_m)\, n(\mathbf{r}_1) \cdots n(\mathbf{r}_m)\right)$$
$$+\int d\mathbf{r}_1\, d\mathbf{r}_2\left[\,\zeta^2(c)\,\chi_c(\mathbf{r}_1 - \mathbf{r}_2)\,\right]\, n(\mathbf{r}_1)\, n(\mathbf{r}_2) + \int \omega\,|\nabla c|^2\, d\mathbf{r}_1$$

$$C_{2(eff)} = \chi_1\,(c)\, C_2^{AA}\,(|\mathbf{r}-\mathbf{r}'|) + \chi_2\,(c)\, C_2^{BB}\,(|\mathbf{r}-\mathbf{r}'|)$$

Correlations in average density

$$\chi^{(3)} = (a\,r + b)\chi(\mathbf{r}_1 - \mathbf{r}_2)\,\chi(\mathbf{r}_1 - \mathbf{r}_3)$$
$$\chi^{(4)} = c\,\chi(\mathbf{r}_1 - \mathbf{r}_2)\,\chi(\mathbf{r}_1 - \mathbf{r}_3)\,\chi(\mathbf{r}_1 - \mathbf{r}_4)$$

modulates average density with conc. →

$$\zeta^2(c) = \frac{u_1}{2}(c - c_0)^2 + \frac{v_1}{4}(c - c_0)^4$$

Nan Wang and N. Provatas, Phys. Rev. Materials (2017)

$$\hat{\chi}(k) = e^{-k^2/2\lambda} \quad \hat{\chi}_c(k) = e^{-k^2/2\lambda_c}$$

Four-Phase Equilibrium Properties

Simple eutectic phase diagram, with a triple-point

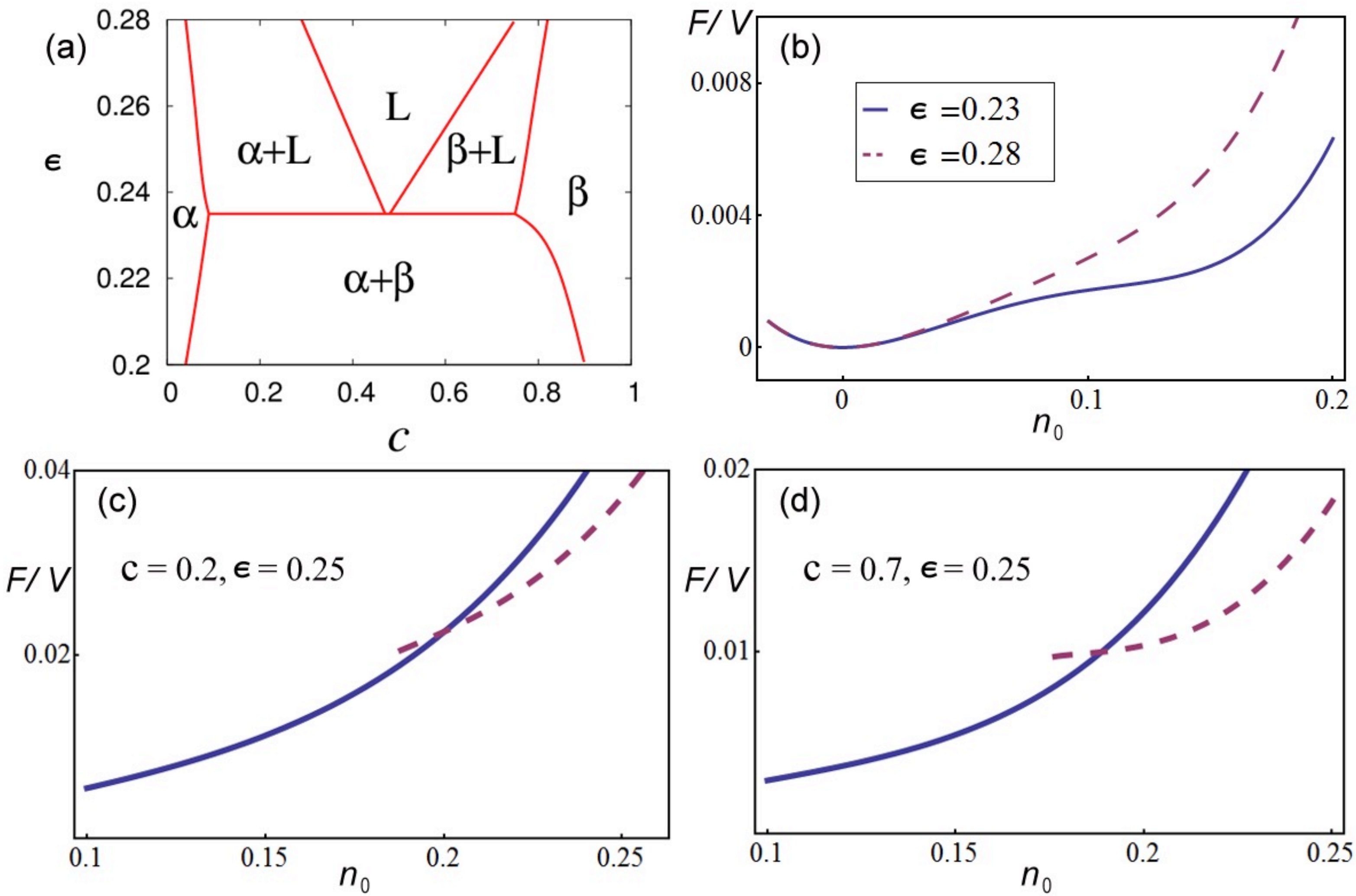

Mushy-Zone Pressure Drop in Confined Liquid Channel

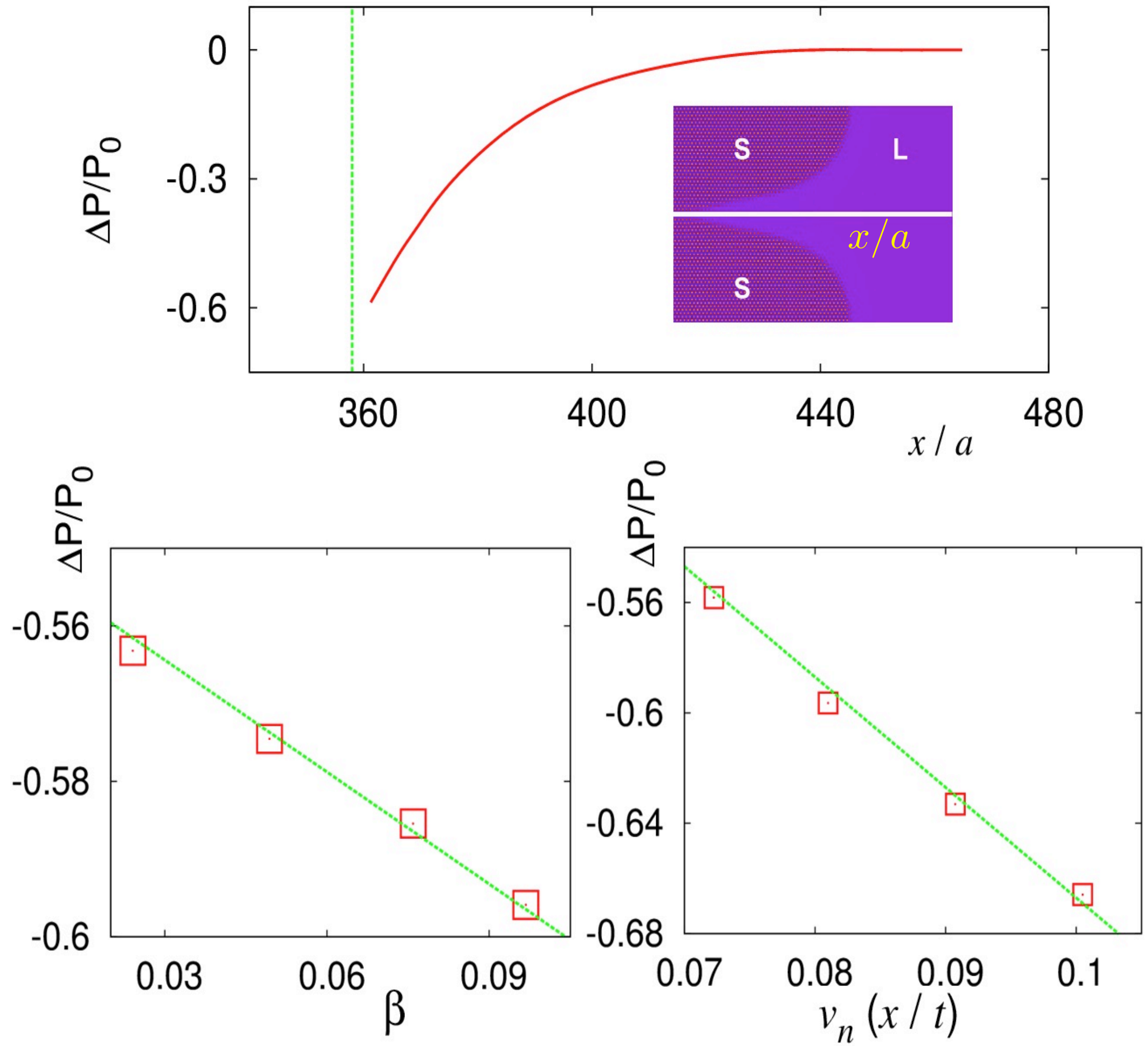

$$\beta = \frac{(\rho_s - \rho_L)}{\rho_L}$$

"Shrinkage factor "

$$v_n$$

Solidification speed

Cavitation & Induced Nucleation Of Carbide Phase Particle

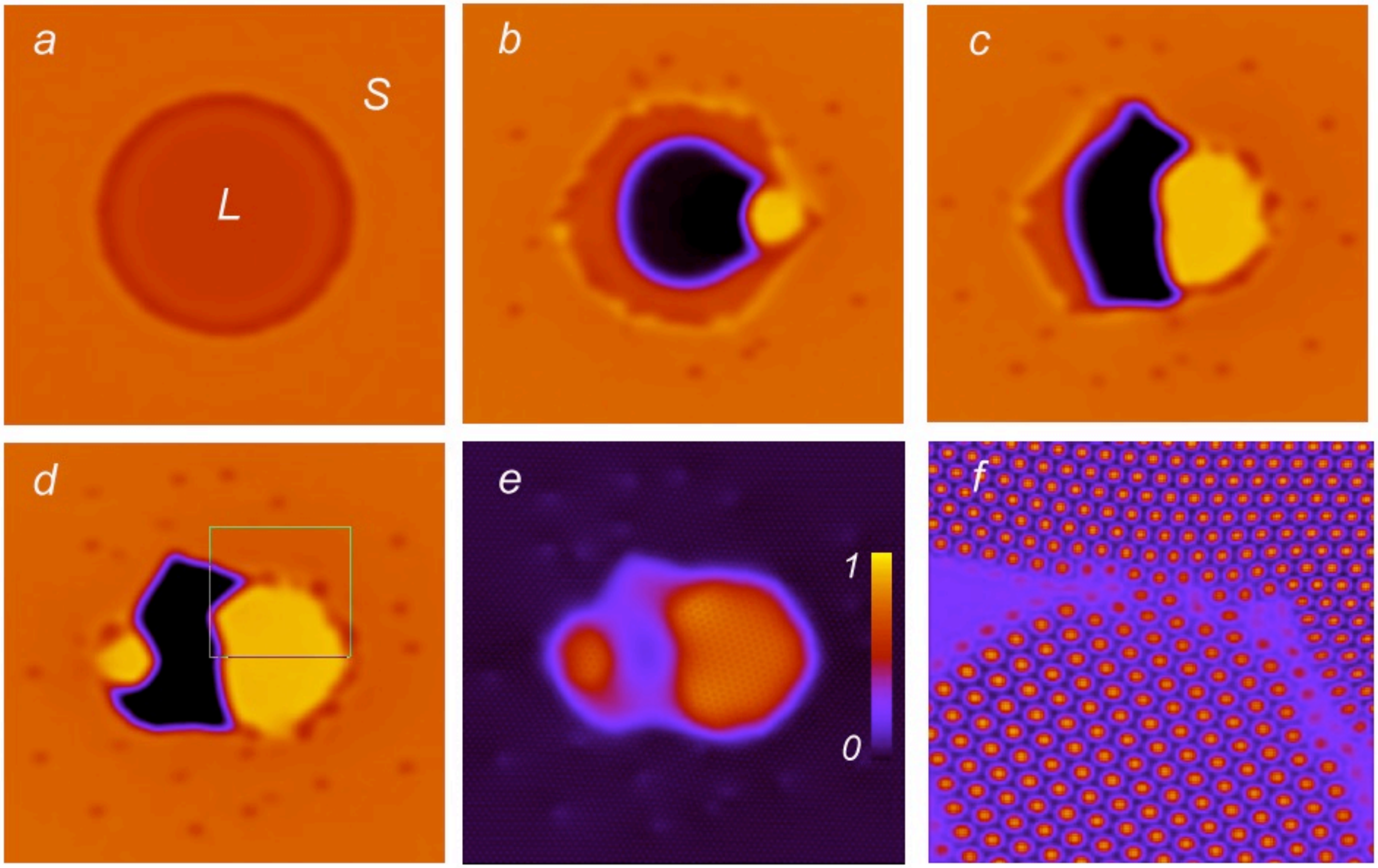

Liquid cavitation promoting the nucleation and growth of the high concentration solid (carbide) phase.

Nan Wang and N. Provatas, Phys. Rev. Materials (2017)

ICME Materials Informatics: Blueprint

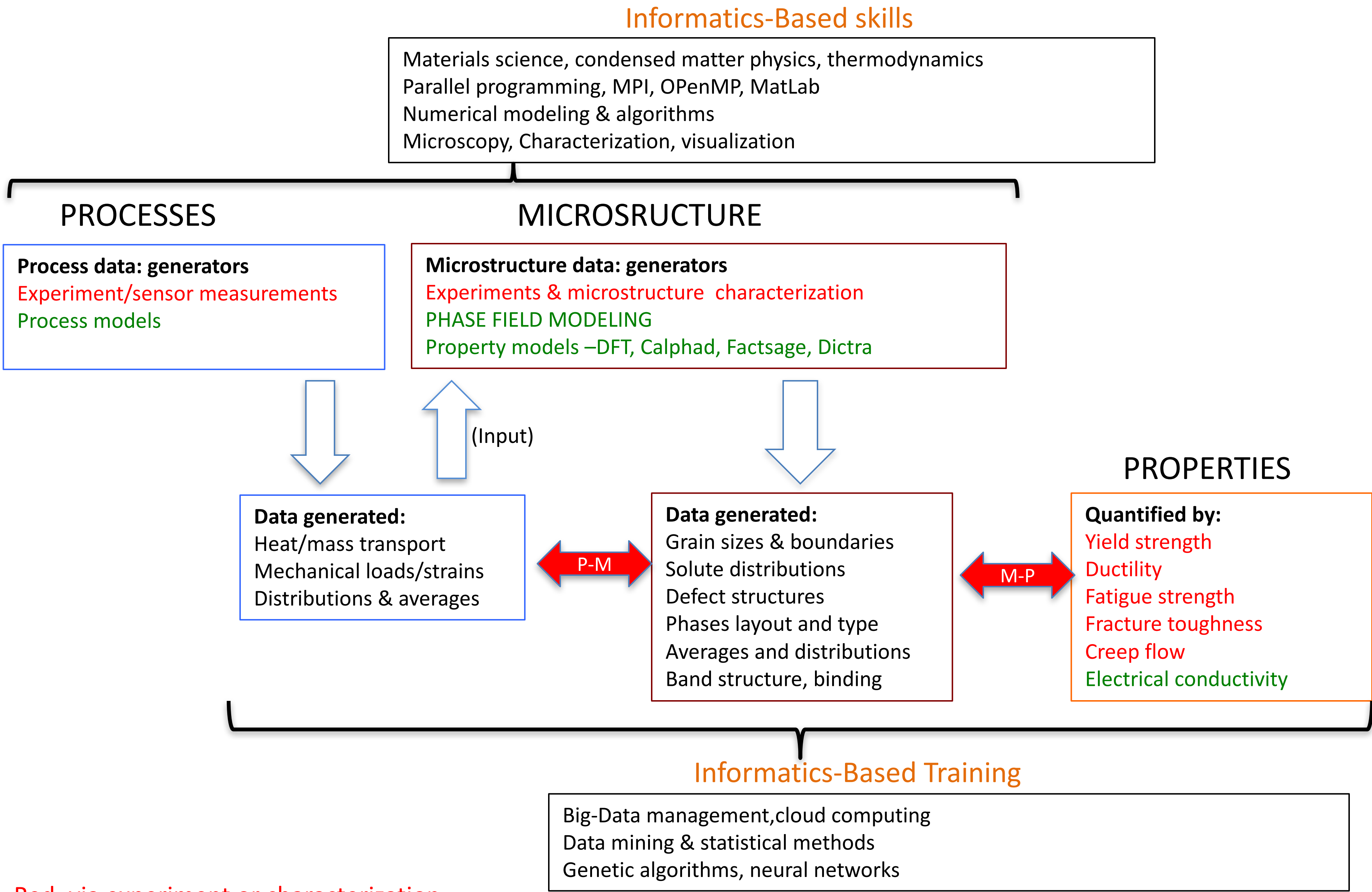

Red=via experiment or characterization
Green=via computational model or theory

Conclusions & Future Outlook

1. PF models: capture the physics of most free-boundary microstructure problems quantitatively

1. PFC models: robust way to include atomic-scale structure and elasto-plasticity to microstructure evolution (elasticity, grain boundaries, dislocations)

2. Outlook:
    1. Generating field theory that unifies all phenomena observed with PFC model under one density field

    2. Consistent coarse graining formalism to generate consistent mseo-scale (PF) theories

3. ICME link with PFC-generated PF models for multi-scale